PERGAMON

Journal of Structural Geology 24 (2002) 193–217

JOURNAL OF STRUCTURAL GEOLOGY

www.elsevier.com/locate/jstrugeo

Ductile fabrics in the zone of active oblique convergence near the Alpine Fault, New Zealand: identifying the neotectonic overprint ☆

T.A. Little[a,*], R.J. Holcombe[b], B.R. Ilg[a]

[a]*School of Earth Sciences; Victoria University of Wellington, Wellington, New Zealand*
[b]*Department of Earth Sciences, University of Queensland, Queensland, 4072 Australia*

Received 12 June 2000; revised 5 April 2001; accepted 23 April 2001

Abstract

The mid-crustal Alpine Schist in central Southern Alps, New Zealand has been exhumed during the past ~3 m.y. on the hanging wall of the oblique-slip Alpine Fault. These rocks underwent ductile deformation during their passage through the ~150-km-wide Pacific–Australia plate boundary zone. Likely to be Cretaceous in age, peak metamorphism predates the largely Pliocene and younger oblique convergence that continues to uplift the Southern Alps today. Late Cenozoic ductile deformation constructively reinforced a pre-existing fabric that was well oriented to accommodate a dextral-transpressive overprint. Quartz microstructures below a recently exhumed brittle-ductile transition zone reflect a late Cenozoic increment of ductile strain that was distributed across deeper levels of the Pacific Plate. Deformation was transpressive, including a dextral-normal shear component that bends and rotates a delaminated panel of Pacific Plate crust onto the oblique footwall ramp of the Alpine Fault. Progressive ductile shear in mylonites at the base of the Pacific Plate overprints earlier fabrics in a dextral-reverse sense, a deformation that accompanies translation of the schists up the Alpine Fault. Ductile shear along that structure affects not only the 1–2-km-thick section of Alpine mylonites, but is distributed across several kilometres of overlying nonmylonitic rocks.

Keywords: Oblique convergence; Transpression; Alpine Fault

1. Introduction

The Southern Alps on the South Island of New Zealand are a key locality for understanding oblique plate convergence in continental crust (Norris et al., 1990; Walcott, 1998). There, oblique-slip on the Alpine Fault is currently exhuming a section of Pacific Plate schists that resided in the middle crust of the Southern Alps orogen only 2–3 million years ago (Adams, 1979; Tippet and Kamp, 1993; Batt et al., 2000). Late Cenozoic plate motions (Sutherland, 1995) and patterns of contemporary strain in the Pacific–Australian plate boundary zone (Beavan et al., 1999) are known from sea-floor spreading and Global Positioning System data. Recent geophysical transects have imaged the crust and mantle (Stern et al., 1997; Molnar et al., 1999), providing a snapshot of the deep structure of the orogen. These data provide a rare opportunity to examine ductile fabric development of naturally deformed rocks in the context of a well-understood kinematic framework (Fig. 1a). Recent work has focused on slip-rates, segmentation, critical wedge mechanics, and paleoseismicity of the Alpine Fault and its bordering mylonite zone (e.g. Norris and Cooper, 1995, 1997; Sutherland and Norris, 1995), but relatively little is known about amounts and styles of deformation affecting deeply exhumed non-mylonitic schists that comprise the bulk of the Alpine Fault's hanging wall.

Numerical modelling and strain-based theoretical studies have used the Southern Alps as a key example of an obliquely convergent orogen — one characterised by strongly asymmetric erosion rates and a non-partitioned style of oblique motion (Mount and Suppe, 1992; Koons, 1994; Braun and Beaumont, 1995; Teyssier et al., 1995; Beaumont et al., 1996; Jiang et al., 2001). These studies make predictions about strain distribution and fabric evolution in obliquely convergent mountain belts. Further progress in understanding the mechanics of these types of plate boundary zones is hindered by a paucity of field data against which such models can be tested. Although much recent work has focused on active tectonics and surface processes, examination of deeper-seated ductile

☆ See "Electronic Supplements" on this journal's homepage: http://www.elsevier.com/locate/jstrugeo

* Corresponding author. Tel.: +64-4-463-5233-8404; fax: +64-4-463-8186.

E-mail address: timothy.little@vuw.ac.nz (T.A. Little).

0191-8141/02/$ - see front matter
PII: S0191-8141(01)00059-1

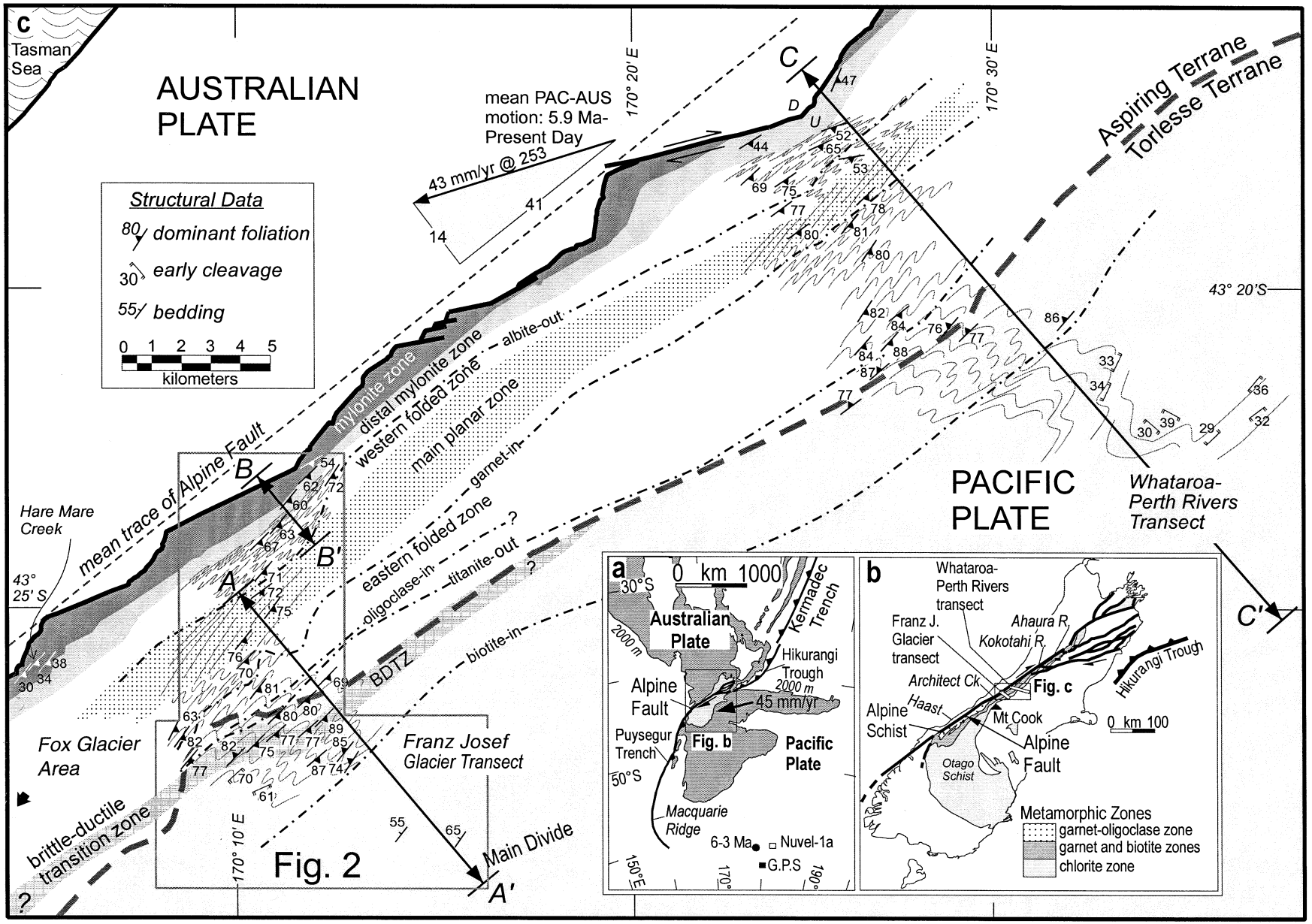
c
Tasman Sea
AUSTRALIAN PLATE
mean PAC-AUS motion: 5.9 Ma-Present Day
43 mm/yr @ 253
41
14
170° 20' E
170° 30' E
C
C'
D
U
Aspiring Terrane
Torlesse Terrane
43° 20'S
Structural Data
dominant foliation
early cleavage
bedding
0 1 2 3 4 5
kilometers
mylonite zone
distal mylonite zone
western folded zone
albite-out
main planar zone
garnet-in
eastern folded zone
oligoclase-in
titanite-out
biotite-in
BDTZ
mean trace of Alpine Fault
Hare Mare Creek
43° 25' S
B
B'
A
A'
PACIFIC PLATE
Whataroa-Perth Rivers Transect
Fox Glacier Area
Franz Josef Glacier Transect
brittle-ductile transition zone
170° 10' E
Fig. 2
Main Divide
a
0 km 1000
30°S
Australian Plate
Kermadec Trench
2000 m
Hikurangi Trough
2000 m
Alpine Fault
45 mm/yr
Puysegur Trench
Fig. b
Pacific Plate
50°S
Macquarie Ridge
6-3 Ma
Nuvel-1a
G.P.S
150°E
170°
190°
b
Whataroa-Perth Rivers transect
Franz J. Glacier transect
Ahaura R.
Kokotahi R.
Hikurangi Trough
Architect Ck
Fig. c
Alpine Fault
Haast
Mt Cook
0 km 100
Alpine Schist
Otago Schist
Metamorphic Zones
garnet-oligoclase zone
garnet and biotite zones
chlorite zone

deformational processes on a neotectonic (<5 Ma) time scale has been less readily forthcoming, chiefly because of the difficulty in sampling appropriate rocks on the earth's surface today. The natural laboratory of the Southern Alps, therefore, provides a special opportunity to enhance our understanding of deformational processes in continental crust.

In this paper we examine deeply exhumed parts of the Alpine Schist (Fig. 1b) to address basic questions about the origin of ductile fabrics in the plate boundary zone between the Pacific and Australian plates. In Pacific Plate rocks uplifted along the Alpine Fault, how do deformational fabrics change with structural depth and distance away from the Alpine Fault? Are there systematic changes in the disposition of foliations across the orogen and, if so, what do they tell us about general processes of oblique convergence? Which fabrics were imprinted during the current phase of mountain building and which were inherited by it? How can we distinguish between inherited and recent fabric contributions? These are some of the issues addressed by this paper.

A major goal of this study is to identify the neotectonic contribution to fabric development in the Alpine Schist. We observed bedrock structures and ductile fabrics along two transects across the central part of the Southern Alps (Fig. 1b), examining microstructures in more than 350 oriented thin-sections. We will argue that a pre-existing foliation was constructively reinforced during the late Cenozoic. A key observation is our local recognition of a fossil brittle-ductile transition in the Alpine Schist, which provides an important structural and thermal marker of late Cenozoic age. New data on fabrics in the Alpine Schist constrain the style of hanging wall deformation above the Alpine Fault, its shear sense, the degree to which it undergoes simple shear vs. irrotational deformation, and the mechanism by which rocks in the central Southern Alps are uplifted. In addition, we synthesize existing work and models on the origin and tectonic significance of the Alpine Schist, placing them in the context of newly emerging geodetic, geophysical and thermochronological data sets. A companion paper (Little et al., 2001) uses finite and incremental strain data to derive a kinematic model for how the middle crust of the Pacific Plate accommodates oblique plate convergence.

2. Tectonic setting and structural framework

Since ~6.4 Ma the Pacific Plate has moved WSW at ~42 mm/year relative to the Australian Plate, resulting in oblique convergence in the Southern Alps (Walcott, 1998). Much of this motion is accommodated by dextral-reverse slip on the SE-dipping Alpine Fault, which regionally strikes ~18–20° anticlockwise of the plate motion vector (e.g. Norris and Cooper, 1995) (Fig. 1c). East of the Alpine Fault, the Pacific Plate is tilted SE to expose a Barrovian metamorphic sequence called the Alpine Schist (Mason, 1962) (Fig. 1b). These rocks, together with the Otago Schist, comprise the Haast Schist belt in the South Island of New Zealand. Garnet–oligoclase zone schists (amphibolite facies) of the Alpine Schist crop out near the fault, whereas chlorite zone semischists (lower greenschist facies) crop out near the Main Divide of the Southern Alps, ~12–15 km to the SE (Grapes, 1995). In between, a series of isograds generally strike subparallel to the Alpine Fault. These are typically more steeply dipping than the fault or are folded (Fig. 3; see also Findlay, 1987; Grapes and Watanabe, 1992) and commonly they coincide with post-metamorphic faults (e.g. Craw, 1998). In map-view they trend obliquely to the Alpine Fault, resulting in changes in the width of metamorphic zones along strike (Fig. 1c; see also Cox and Findlay, 1995). We interpret these relationships as indicating that the metamorphic peak in the Alpine Schist occurred prior to the current phase of oblique convergence, and that the isograd structure does not necessarily reflect the present thermal structure of the orogen. Today, the near-surface geothermal gradient east of the Alpine Fault is >60°C/km, a high value that reflects a dynamic steady-state between uplift-related advection of heat, and erosion and conductive cooling near the surface (Koons, 1987; Shi et al., 1996). The modern brittle-ductile transition zone is probably <10 km deep (Leitner and Eberhart-Phillips, 1998).

The intensity and multiplicity of foliation development increases structurally downward through the Alpine Schist from incipiently cleaved 'semischists' preserving original bedding (textural zone IIa of Bishop, 1972) near the Main Divide, to polydeformed, thickly segregated schists (textural zone IV) within a few kilometers of the Alpine Fault (Fig. 2). Within ~1–2 km of the fault, the Alpine Schist consists of mylonites with dextral-reverse shear fabrics (Sibson et al., 1981). The mylonitic foliation dips ~25–60° SE, subparallel to the Alpine Fault. The mylonites grade structurally upward into a ~0.4–1-km-thick zone of protomylonitic rocks ('curly schists'). We refer to this ~0.4–1-km-thick that we refer to as the distal mylonite zone. The rest of the Alpine Schist is nonmylonitic and (structurally beneath the semischistose rocks) is dominated by a near-vertical foliation. This 'Alpine foliation' strikes

Fig. 1. (a) Index map (inset) showing location of Alpine Fault, and stage pole for Pacific–Australia plate motion between 6 and 3 Ma (black circle from Walcott, 1998). Contemporary Euler pole positions include the <3 Ma estimate of Nuvel-1a (DeMets et al., 1994) (white square) and a recent G.P.S.-derived result (black square). (b) Map of South Island, New Zealand showing selected tectonic and metamorphic features and location of the two structural transects. (c) Simplified geological map of a central part of the Southern Alps, near Franz Josef Glacier, showing the Alpine Fault, metamorphic isograds and selected structural data in the Alpine Schist. See (b) for location. Relative plate motion vector (arrow) is averaged over the last 5.9 m.y. for a site near Franz Josef Glacier using rotation parameters in Walcott (1998). The Alpine Fault trace is from Norris and Cooper (1995).

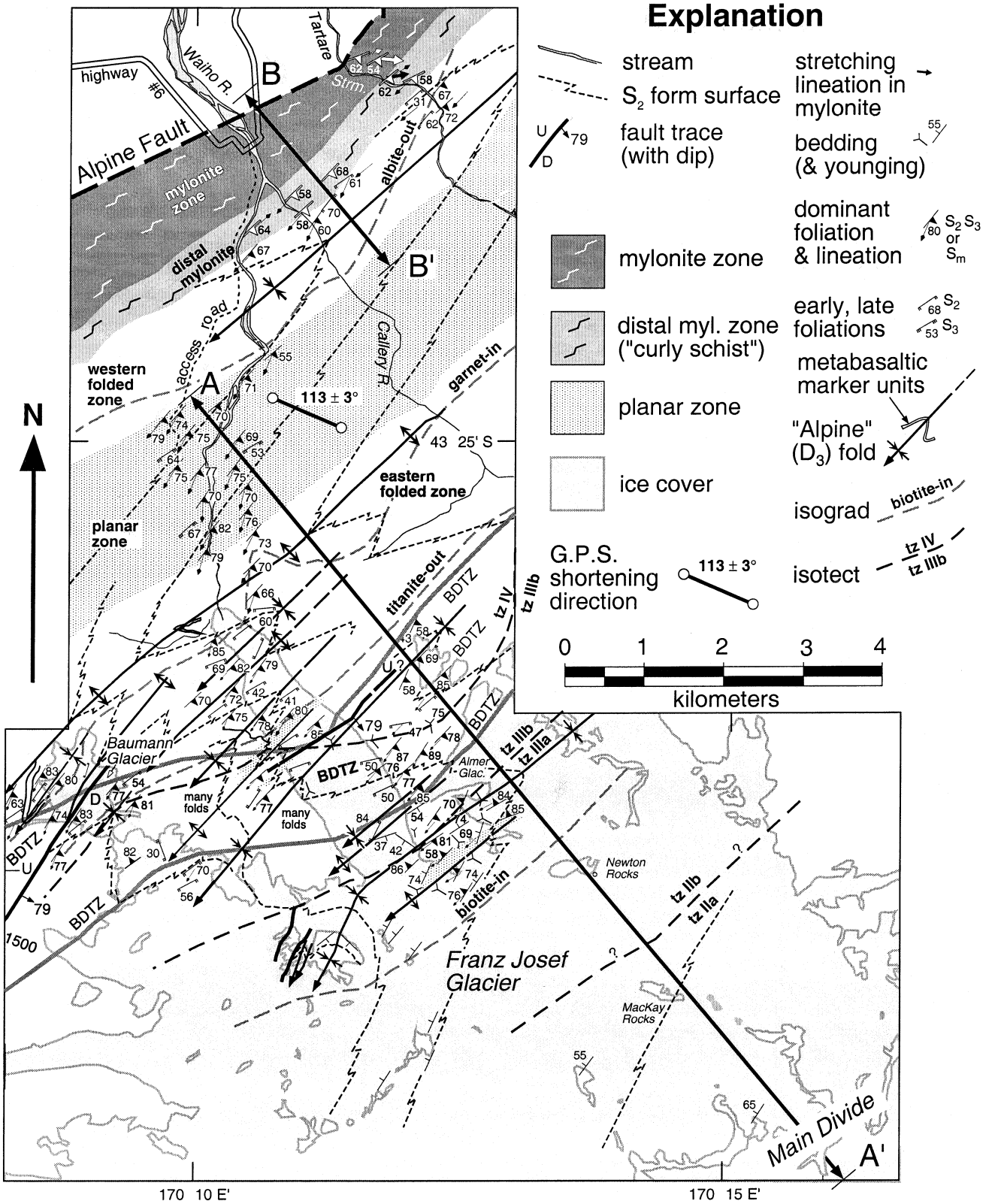

Fig. 2. Bedrock structural geology of the Alpine Schist near Franz Josef Glacier. See Fig. 1c for location. Textural zones (tz) in meta-psammitic rocks are as defined in Bishop (1972) and Norris and Bishop (1990). Brief definitions: tz I, unfoliated sandstone; tzIIa, incipiently cleaved rock; tzIIb, well-cleaved rock retaining abundant relict detrital grains; tzIIIa, incipiently segregated schist; tzIIIb, finely segregated schist with few or no relict detrital grains; and tzIV, thickly segregated schist. Trace of Alpine Fault is from Norris and Cooper (1995). Bedding attitudes near the Main Divide are from Gunn (1960). See Grapes and Watanabe (1992) for description of biotite-in, garnet-in, and albite-out isograds. Titanite-out isograd (this study) marks the prograde reaction causing titanite to be replaced by ilmenite. BDTZ denotes location of exhumed (fossil) late Cenozoic brittle-ductile transition zone recognised as a part of this study.

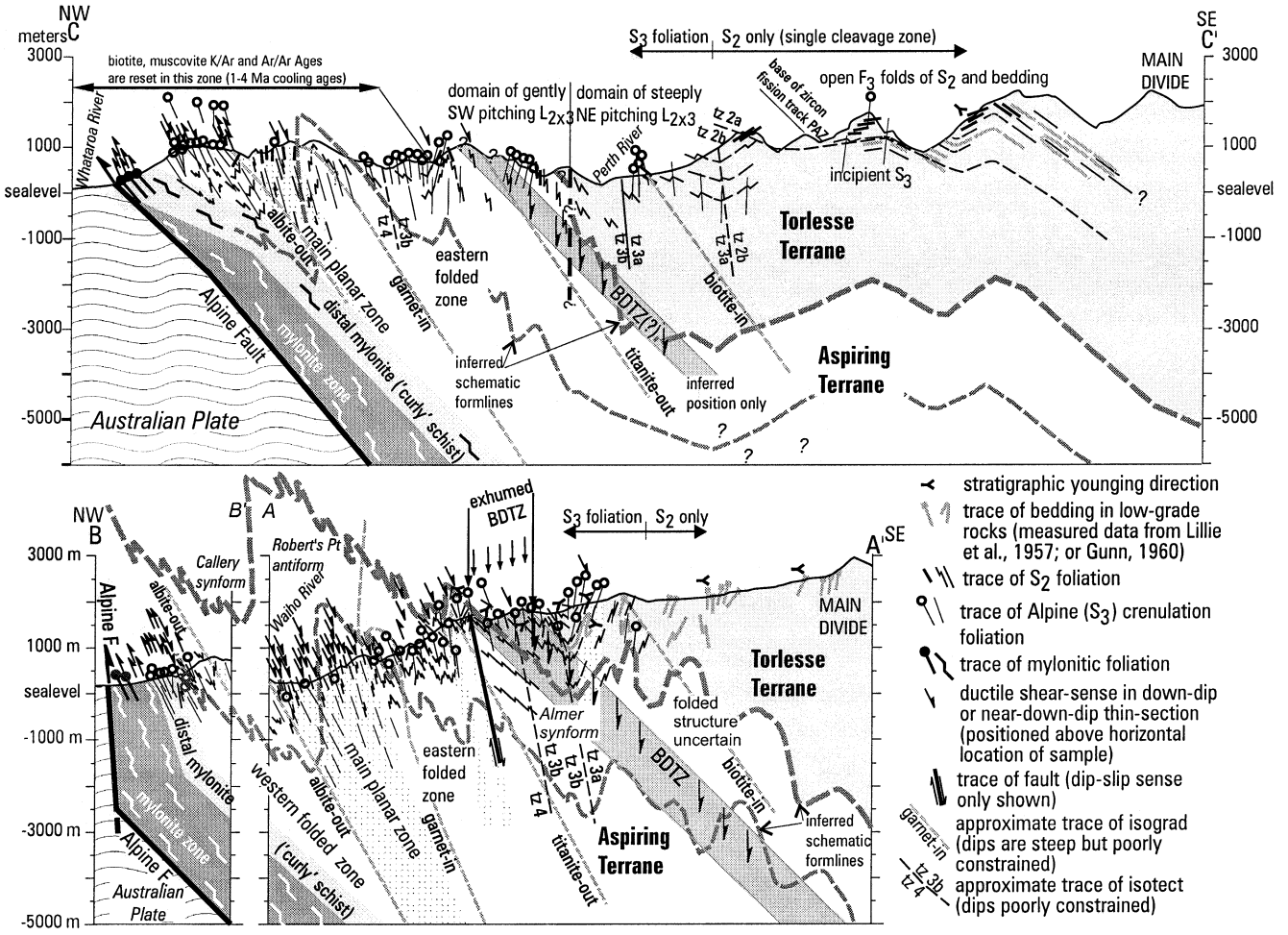

Fig. 3. Structural cross-sections (no vertical exaggeration). See Figs. 1c and 2 for location. A–A′ and B–B′, Franz Josef Glacier–Waiho River; C–C′ Whataroa–Perth Rivers. See Fig. 2 for explanation of patterns. Note that B–B′ samples a steep, strike-slip segment of the Alpine Fault near the surface, hence the apparent kink at depth.

NNE, about 15° discordant to the more easterly striking Alpine Fault. As pointed out by Holm et al. (1989), the foliation is approximately orthogonal to the direction of maximum geodetic shortening rate (Fig. 2).

Near Franz Josef and Fox Glaciers, the Alpine Schist can be differentiated into two lithic assemblages (Fig. 2). Adjacent to the Alpine Fault is a unit of dark grey pelitic schist and lesser psammite that is locally interbedded with ~1–20-m-thick units of metabasalt and metachert. Grapes et al. (1998) correlate this unit with the Aspiring Terrane of Norris and Craw (1987). The structurally higher Torlesse Terrane is dominated by thick-bedded sequences of psammitic schist containing relatively minor pelitic interbeds, ~1–10 m thick. The Alpine foliation and isograds appear to overprint the contact between these units. This contact, together with an early cleavage that we call S_2, is deformed into kilometre-wavelength folds. Their hinges plunge moderately SW and contain the Alpine foliation (our S_3) as an axial planar fabric (e.g. Lillie et al., 1957; Gunn, 1960; Grindley, 1963; Findlay, 1987).

Due to recent isotopic resetting of these rapidly exhumed rocks, dating the Barrovian metamorphism in the Alpine Schist using thermochronometers has proved to be a difficult task, but workers are unanimous in concluding that the thermal peak predates the post-Pliocene phase of oblique convergence. Some have argued for peak metamorphism at ~100–120 Ma (e.g. Grapes, 1995; Walker and Mortimer, 1999), others at ~68 Ma (Chamberlain et al., 1995), and still others have suggested that it could be as young as 15–20 Ma (Findlay, 1987; Holm et al., 1989; Batt et al., 2000). Regardless of which may be correct, the Alpine Schists were subject to a period of sustained deep burial prior to the modern phase of oblique convergence and uplift. Reset fission-track ages of apatite and zircon, of <1 Ma and Ar–Ar ages of biotite, muscovite, and locally hornblende of 1–3 Ma record cooling and exhumation of the Alpine Schist from temperatures locally c. 500°C and depths of 20–30 km during the present phase of rapid uplift (Adams, 1981; Tippet and Kamp, 1993; Chamberlain et al., 1995; Batt et al., 2000). Thus at least some uplift-related ductile deformation is likely to have occurred at deep levels of the Alpine Schist during the past several m.y. (Holm et al., 1989). We

cannot identify this neotectonic strain increment, however, until we understand the sequential development of fabrics in the Alpine Schist.

3. Temporal superposition of fabrics in the Alpine Schist

3.1. Oldest preserved foliations

Microstructural and mesoscopic observations reveal evidence of two ductile fabrics that predate the Alpine foliation (Table 1). Aspiring Terrane rocks preserve evidence for the oldest of these. This S_1 fabric can be locally recognised where it wraps around F_2 fold closures (e.g. Fig. 4a). Microscopically, it is preserved inside biotite and, less commonly, garnet porphyroblasts, as F_2-microfolded inclusion trails (Figs. 5d and 6a). The early foliation (S_2) is well preserved in both the Torlesse and Aspiring Terranes, and is locally the dominant foliation in the rocks. F_2 folds of S_1 bedding and veins are all isoclinal with strongly attenuated limbs (Fig. 4a and b). This strongly laminated fabric is crenulated by the younger Alpine foliation (S_3). The presence of an extra ductile fabric in the Aspiring Terrane relative to the structurally adjacent Torlesse Terrane, and our observation that strongly rodded broken formations occur along their contact suggest that their boundary is a ductile shear zone (e.g. Norris and Craw, 1987).

3.2. Fabric development during and after peak metamorphism of the Alpine Schist

Microtextures indicate that peak metamorphism of the Alpine Schist took place during formation of the Alpine foliation (S_3), but that most mineral species remained stable through periods of subsequent growth and deformation until late Cenozoic termination of the mylonitic deformation. Uplift and erosion rates on the Alpine Fault are inferred to be 8–10 mm/year in the central Southern Alps (Bull and Cooper, 1986; Simpson et al., 1994), thus this termination would have taken place at ~1 Ma if the brittle-ductile transition zone has a steady-state depth of 8–10 km. In nonmylonitic rocks, we refer to the peak metamorphic phase of deformation accompanying initial crenulation, porphyroblast nucleation and Alpine foliation development as D_3. We will argue that ductile deformation post-dating and modifying the Alpine foliation includes a final increment acquired during the late Cenozoic (D_4). In most cases microstructures related to late-D_3 stages of crenulation tightening cannot be distinguished from ones forming during late Cenozoic oblique convergence, because the two flattening increments were acquired under similar metamorphic conditions and the latter constructively reinforced the former. For this reason, we will refer to the cumulative imprint of post-D_3 ductile deformation with the deliberately vague term, D_{3-4}. Note that D_3 and D_4 may have been separated in time by as much as 100 m.y.

Biotite, plagioclase, muscovite and prograde-zoned almandine garnet grew during D_3. The same minerals, with the possible exception of garnet, grew during D_{3-4} in dilatation sites such as strain shadows, and they also define the high-strain mylonitic fabric (S_m) near the Alpine Fault. Thermobarometric work in the central Southern Alps indicates that peak temperatures in the nonmylonitic part of the Alpine Schist reached 480–620 ± 50° at pressures of 8–11 kbars (Cooper, 1980; Grapes, 1995). Prograde zoning of garnet in both temperature and pressure suggest that the Alpine metamorphism progressed during a phase of crustal thickening, taking some rocks to depths of up to 40 km (e.g. Cooper, 1980; Grapes, 1995; Vry et al., 2001). Some have inferred that this metamorphism and convergence took place in the Jurassic–Cretaceous, prior to the mid Cretaceous initiation of rifting in New Zealand. Up to 14 km of denudation is inferred to have affected the Alpine Schist prior to the late Cenozoic (Cooper, 1980; Tippet and Kamp, 1993; Grapes, 1995). Recent Sm–Nd dating and thermobarometry, however, indicating growth of garnet cores in the Late Cretaceous, coeval with regional extension in New Zealand, followed — much later — by further garnet growth and in the Cenozoic, during conditions of increasing P and T (Vry et al., 2001). Relatively clear, late-stage (Cenozoic?) overgrowths on garnet are especially common in the garnet–oligoclase zone (Figs. 5a and 6b). These are commonly partially replaced or microveined by chlorite, but pervasive greenschist–facies retrogression generally only affects cataclastic rocks within ~30 m of the Alpine Fault (Fig. 5a) (Sibson et al., 1981).

In nonmylonitic rocks of the garnet and garnet–oligoclase zones, coarse garnet and biotites commonly overgrow graphite-rich laminae that are parallel to S_2 (Fig. 5c and d). The early foliation can be traced from the matrix into the porphyroblasts where S_2 is preserved as inclusion trails composed of graphite, quartz, ilmenite, epidote, muscovite and calcite. In D_3-crenulated rocks, these trails are straight in the cores of some garnet porphyroblasts, and become curved or crenulate near grain margins, indicating that garnet growth was early to syn the D_3 crenulations (Fig. 6b). Further flattening (D_{3-4}) post-dating garnet growth is indicated by wrapping of the external (S_3) foliation around the grains, by strain shadows abutting them, and by extension fractures splitting garnet at a high angle to S_3, some of which have undergone bookshelf tiling (Figs. 5b and d and 10c).

Biotite shows many phases of syndeformational growth, starting before the onset of D_3, with the oldest continuing and the youngest after inception of the Alpine crenulation foliation. Biotite prisms in some crenulated rocks contain straight to slightly curved inclusion trails of the externally crenulated S_2 fabric, indicating early syntectonic growth in D_3 (Fig. 5c and d). Elongate blades aligned parallel to S_3, and triangular infills of dilation sites in the polygonal arcs of white mica crenulations, also record syn D_3 growth (Fig. 5d). Predominantly late- to post-D_3 nucleation of biotite is indicated by the abundance of porphyroblasts that contain

Table 1
Spatial and temporal summary of Alpine Schist ductile fabrics (near Franz Josef Glacier and in Whataroa and Perth River Valleys)

Inferred deformation age	Identifiable fabric element	Deformation phase	**Northwest** Mylonite and distal mylonite (curly) zones	Western folded zone	Main planar zone	Eastern folded zone	**Southeast** Single cleavage zone
Older							
	Bedding (S_0)		Inconspicuous, except for metachert, metabasalt layers	Inconspicuous, except for metachert, metabasalt layers	Inconspicuous, except for metachert, metabasalt layers	Conspicuous (graded beds)	Dominant
Jurassic or Cretaceous	S_1	D_1	Generally not preserved	Remnant S_1 in rare F_2 closures and as folded inclusion trails in porphyroblasts	Remnant S_1 in rare F_2 closures and as folded inclusion trails in porphyroblasts	Absent in Torlesse Terrane	Absent in Torlesse Terrane
Jurassic or Cretaceous	Early foliation (S_2)	D_2	S_2 preserved as inclusion trails in porphyroclastic garnets	S_2 is laminated foliation shortened by later (F_3) crenulation folds	Laminated S_2 is dominant foliation; occurs on steeply dipping limbs of Alpine (F_3) folds	S_2 is shortened by later (F_3) crenulation folds	S_2 rough cleavage is sole fabric; subparallel to bedding except in F_2 hinges
Mid Cretaceous to early Miocene	Alpine foliation Alpine foliation (S_3)	D_3		Peak metamorphic crenulation foliation	Reinforcement of steep S_2. F_3 crenulations preserved locally	Peak metamorphic crenulation foliation	Mostly absent or weak. F_3 crenulations preserved locally
Late Cenozoic	Alpine foliation	D_4	Composite fabric, S_3, is transposed into younger mylonitic foliation (S_m)	Tightening of S_3 (microboudinage, book-shelf sliding, rotation, strain shadow enhancement)	Reinforcement of S_2 (microboudinage, book-shelf sliding, rotation, strain shadow enhancement)	Tightening of S_3 (microboudinage, book-shelf sliding, rotation, strain shadow enhancement)	Absent
Late Cenozoic	Brittle-ductile shears (S_{bds})	D_4	Absent	Absent	Absent	Zone of dextral E-side-down brittle-ductile shears cross-cutting S_3	Absent
Late Cenozoic	Mylonitic foliation (S_m)	D_4	Mylonitic fabric with abundant, often conjugate, extensional S/C' bands	Reinforces S_3 foliation at western edge of zone	Absent	Absent	Absent
Younger							
			Aspiring Terrane garnet–oligoclase zone	Aspiring Terrane mostly garnet–oligoclase zone	Aspiring Terrane mostly garnet zone	Aspiring and Torlesse Terrane biotite ± garnet zones	Torlesse Terrane mostly chlorite zone

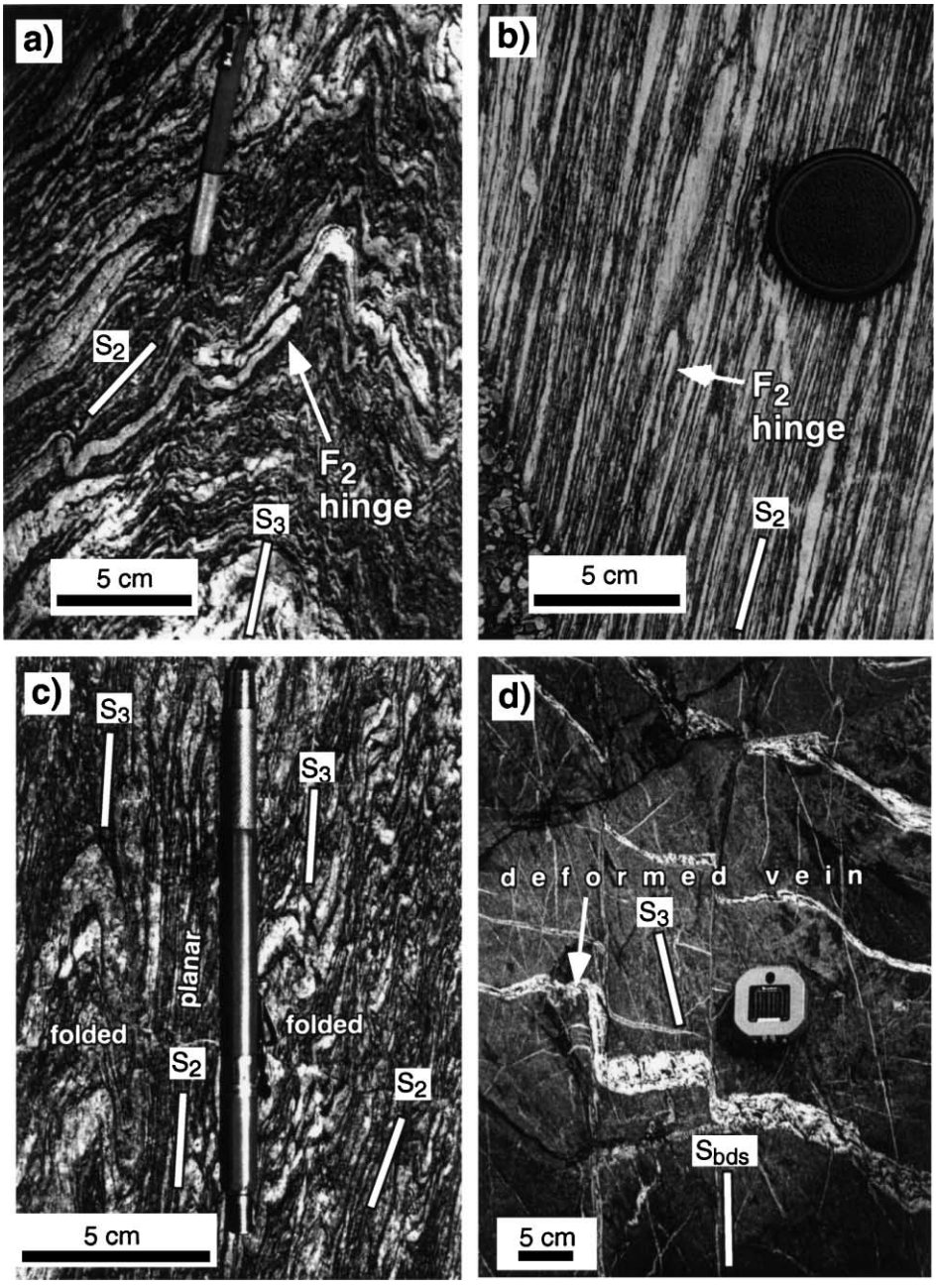

Fig. 4. Outcrop photographs of deeper, nonmylonitic parts of the Alpine Schist. (a) S_3 crenulation fabric in Aspiring Terrane pelite deforming the strongly segregated early foliation, S_2, in garnet–oligoclase zone rocks of the western folded zone. Note lenticular quartz boudin near left edge and isocline in centre indicating transposition in the S_2 fabric. b) Steepened S_2 fabric in main planar zone at Franz Josef Glacier (garnet zone). Note similar transposition structures as in (a). (c) S_3 crenulation fabric deforming S_2 at Franz Josef Glacier (biotite zone). Note centimetre-scale alternation of folded and planar fabric zones, and weakly differentiated nature of S_3 compared with the strongly laminated S_2. (d) Late Cenozoic brittle-ductile shears in exhumed brittle-ductile transition zone (BDTZ) at Franz Josef Glacier (biotite zone). View is of a vertical face, looking NE parallel to strike of the shears and the Alpine Fault. Note truncation of S_3, and brittle to ductile offset of quartz–carbonate veins with down-to-the-SE sense of throw.

microfolded inclusion trails (Figs. 5d and 6c). Shortening increments that post-date biotite nucleation are indicated by deflection of the external foliation around porphyroblasts and by the smaller interlimb angle of F_3 microfolds in the matrix relative to those trapped inside porphyroblasts (Fig. 5d). Where S_2 is the dominant foliation, variably oriented biotite laths overgrow S_2-parallel graphite-rich laminae as well as sparse S_3 crenulations (Fig. 5c). Post-growth (D_{3-4}) flattening is indicated by microboudinage or kinking of biotite laths in which (001) is at a ~90° angle to the foliation; and by spectacular rigid-body rotation and bookshelf-style microfaulting of inclined laths (Figs. 6e and 10b). Biotite syntectonic with D_{3-4} infills strain shadows abutting garnet, ilmenite, and biotite grains, syntaxially heals microboudin fragments, and stitches together cleavage microfaults between bookshelf-sliding packets (Fig. 5c). In

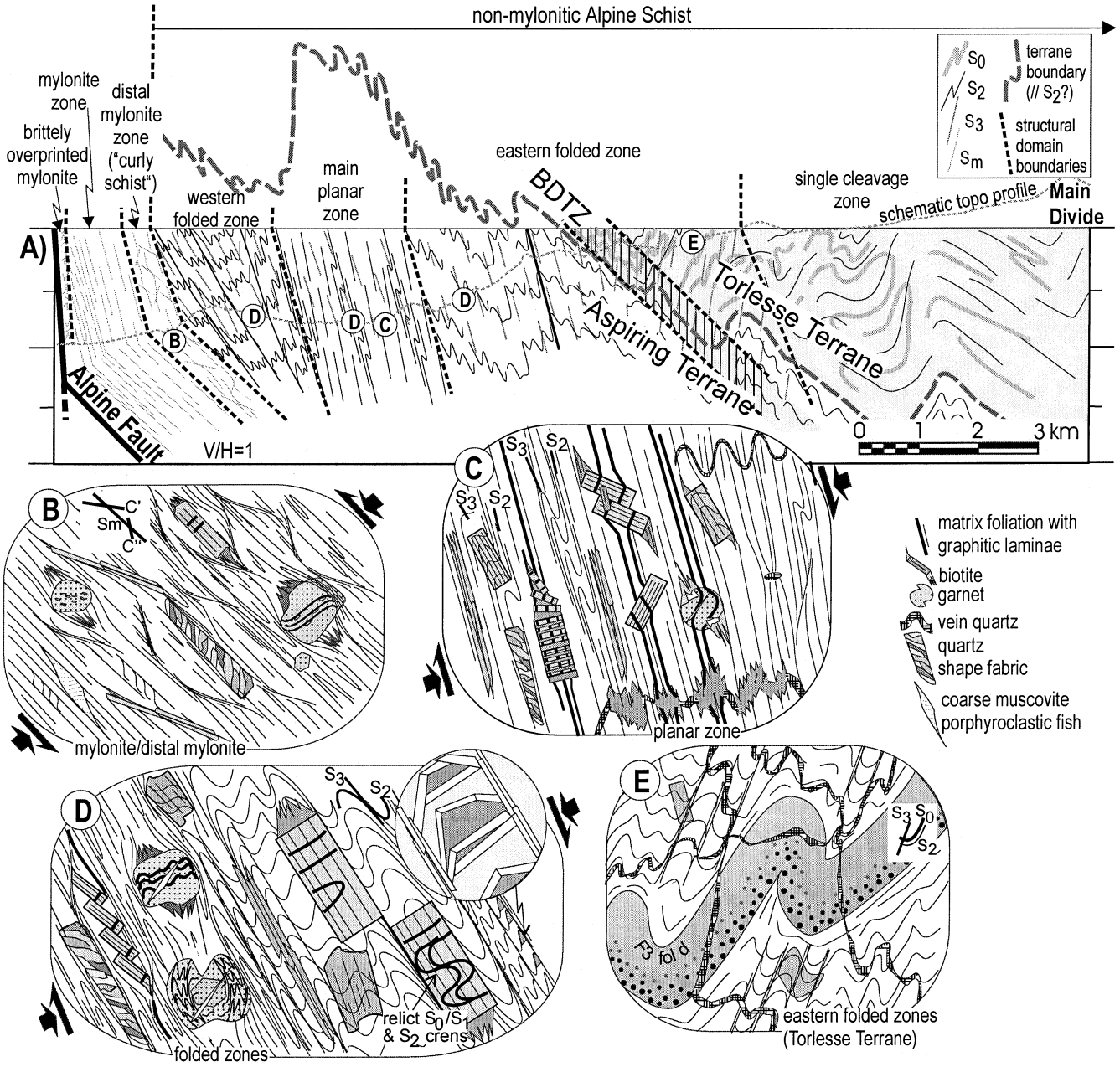

Fig. 5. (a) Schematic NW–SE cross-section adjacent to the Alpine Fault in the Franz Josef Glacier area showing ductile fabrics in the Alpine Schist. Typical microstructures in the Alpine Schist are depicted in schematic insets for each type of zone: (b) mylonite and distal mylonite zones; (c) planar zones (Alpine fold limb); and folded zones in (d) Aspiring Terrane and (e) Torlesse Terrane rocks.

zones of steeply dipping, planar S_2. Biotite laths enclosing relict F_3 crenulations are commonly surrounded by an external matrix with graphitic laminations that lack any such microfolds (Fig. 6c). We believe that this relationship records decrenulation of the planar fabric zones during a post-porphyroblast phase of layer-parallel extension.

3.3. Late Cenozoic mylonitic fabric

Stability of biotite, muscovite, and oligoclase during the late Cenozoic mylonitization is demonstrated by their growth along both S and C' planes in the Alpine mylonite zone and by their infilling of strain shadows in those rocks. Ilmenite in the mylonite zone is rimmed or replaced by retrogressive titanite. Where present, K-feldspar porphyroclasts are recrystallized to a core-and-mantle structure or rimmed by myrmekite, as is consistent with deformation at ~500°C (Passchier and Trouw, 1996) and with ^{40}Ar–^{39}Ar ages on hornblende of 3–5 Ma (Chamberlain et al., 1995). Most garnet in both the main and distal mylonite zone are coarse (3–15 mm in diameter) and porphyroclastic (Fig. 5b). These contain straight to curved S_2 inclusion trails like those in nonmylonitic schist, but these trails are oriented at various angles to the foliation because of a

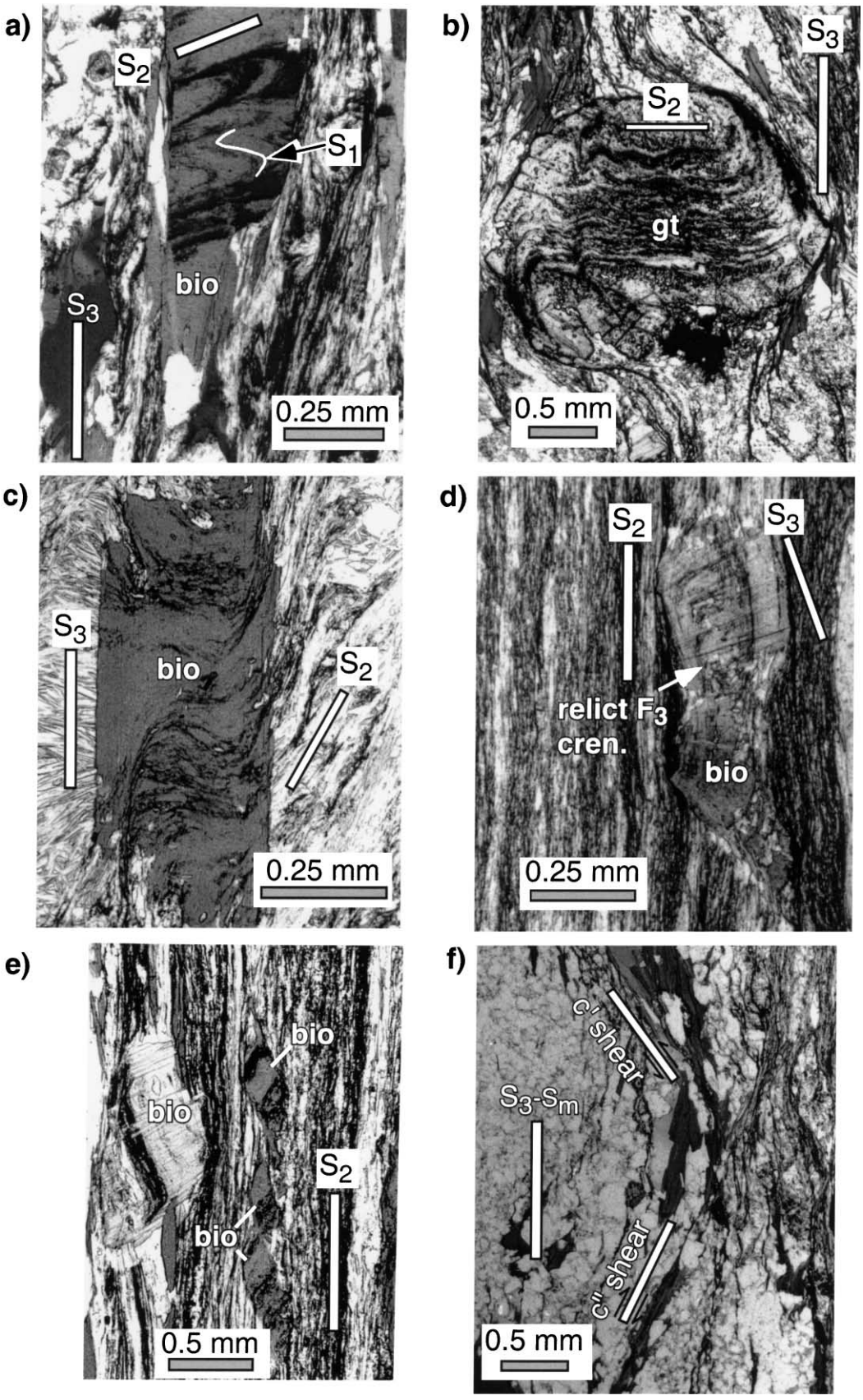
a)
S2
S1
bio
S3
0.25 mm
b)
S3
S2
gt
0.5 mm
c)
S3
bio
S2
0.25 mm
d)
S2
S3
relict F3
cren.
bio
0.25 mm
e)
bio
bio
S2
bio
0.5 mm
f)
c' shear
S3-Sm
c'' shear
0.5 mm

non-uniform shear-induced rotation of the differently shaped garnet grains. Porphyroclastic garnet is strongly wrapped by the mylonitic foliation (S_m) and have elongate strain shadows. Clear, euhedral rims are enriched in Mn and Ca relative to the sieve-textured cores. These rims may overgrow preexisting strain shadows or include strongly wrapped segments of the mylonitic foliation, textures indicative of syn- to late-mylonitic (i.e. late Cenozoic) growth (Fig. 5b). Optically, the rims resemble other coexisting clear euhedral garnet <0.5 mm in diameter (Fig. 5b). The fine-grained garnet are only slightly wrapped by the foliation and typically have thin (or absent) strain shadows infilled with chlorite + quartz. These textures support the inferences of Grapes (1995), Upton (1995), Grapes and Vry (1999), and Vry et al. (2001) that some growth of garnet accompanied the mylonitisation (but see also Prior, 1993). Estimates for the conditions of mylonitisation are 500–550° and 6–8 ± 1 kb in the Franz Josef–Fox Glaciers region (Grapes, 1995; Grapes and Vry, 1999).

4. Spatial zonation of ductile fabrics in the Pacific Plate

Across the SE-tilted section of Pacific Plate rocks, ductile fabrics preserved at high structural levels near the Main Divide are overprinted by successively younger ductile fabrics with increasing structural depth towards the Alpine Fault (Table 1).

Chlorite zone Torlesse Terrane rocks near the Main Divide contain bedding and a single ductile fabric, the early foliation (S_2). In psammites, this foliation is a rough cleavage anastomosing around detrital grains that are modified by pressure solution and fringed by mica beards. We refer to this as the 'single cleavage zone' (Fig. 3, C–C'). S_2 is bedding-subparallel except in the hinges of isoclinal F_2 folds. In upper Perth River, the bedding-cleavage intersection lineation ($L_{0\times2}$) plunges 20–25° towards ~263, parallel to a D_2 elongation lineation defined by stretched detrital grains and fibrous gashes. In the single cleavage zone, S_2 is broadly warped across Alpine (D_3) folds, and commonly it is gently dipping; however, in the neve of the Franz Josef Glacier, bedding and S_2 dip steeply to the NW (Fig. 3, A–A′).

Farther down-section, near the biotite isograd, the Alpine crenulation foliation is imprinted across S_2 (Figs. 3 and 5a). Alpine (D_3) folds deform the early foliation (S_2), which lacks biotite (Fig. 4a). Alpine folds range in size from millimetre-spaced crenulations to kilometre-wavelength folds that typically have steeply dipping or structurally inverted short limbs (Figs. 2 and 3). Their hinges generally plunge SW. The Alpine foliation, S_3, is axial planar to these asymmetric folds. The hinges and long limbs of folds dip gently and contain abundant parasitic folds. We refer to this as the eastern folded zone. There, Alpine folds have straight limbs, slightly thickened hinge zones, and interlimb angles of 30–60° (Fig. 5e). Psammite beds have a class 1c dip-isogon pattern, whereas pelites have a class 3 pattern, typical of flattened buckle folds (Ramsay, 1967). A distinct intersection lineation ($L_{2\times3}$) is parallel to the hingelines of these folds. F_2 folds of bedding are refolded into type 3 (coaxial) interference patterns by F_3 (Ramsay, 1967). Quartz and quartz–carbonate veins are ptygmatically buckled in S_3. Biotite typically occurs as small porphyroblasts of late syn- to post-D_3 age, or as isolated plates parallel to S_3.

With increasing structural depth, S_2 becomes more strongly segregated in appearance, especially in Aspiring Terrane pelites of the garnet zone. At and below textural zone IIIb, just below the biotite-in isograd, relict detrital quartz grains are entirely recrystallised, and the abundance of centimetre-thick quartz veins, subparallel to S_2, increases markedly. These rocks typically contain 1–3-mm-thick quartz-rich laminae (Q domains) alternating with darker, mica and graphite-rich laminae (M domains). This layering reflects pressure solution and diffusive mass transfer of quartz away from the M domains during D_2. Metamorphic segregation also enhances the younger Alpine foliation (S_3), but to a much lesser degree (Fig. 4c). This contrast in differentiation highlights a fundamental difference between the early and Alpine fabrics. The early foliation (S_2) is a transposition fabric recording, we believe, a very large finite strain. Psammitic interbeds within pelitic sequences, for example, are strongly extended along S_2 to form trains of isolated lenticular boudins. The Alpine foliation, by contrast, is a spaced crenulation cleavage that reflects, at most, a moderate shortening of S_2.

On the steep limbs of the asymmetric Alpine folds, S_2 has been steepened into subparallelism with mean S_3. There, S_2 is retained as the dominant foliation (Fig. 4b and c). Most D_3 crenulations originally present in these limbs have been decrenulated due to layer parallel extension in S_2. We refer to fold limbs preserving the S_2 fabric as planar zones. In both transects, a 1–2-km-thick planar zone occurs ~3 km from the Alpine Fault in garnet-bearing pelitic rocks

Fig. 6. Photomicrographs of key microstructures in the Alpine Schist (plain light). All thin sections were cut perpendicular to the $L_{2\times3}$ intersection lineation. 'bio' and 'gt' refer to biotite and garnet. (a) Biotite porphyroblast preserving D_2-crenulated S_1 foliation as graphitic inclusion trails. (b) Almandine-rich garnet with straight to curved inclusion trails indicative of syntectonic growth during development of Alpine fabric (western folded zone). Note clear (late Cenozoic?) rims overgrowing pre-existing crenulation microfolds. (c) Biotite lath overgrowing pre-existing D_3 microfold (eastern folded zone). (d) Helicitic biotite porphyroblast surrounded by decrenulated matrix that lacks microfolds (main planar zone, Franz Josef Glacier). (e) Post-nucleation (D_{3-4}) rigid-body rotation and bookshelf-sliding of biotite laths (main planar zone, Franz Josef Glacier). Note both forward and backward rotation of laths relative to foliation, which is preserved as inclusion trails in the porphyroblasts. (f) Conjugate development of oblique (extensional) shear bands in transition zone between the distal mylonite zone and the nonmylonitic Alpine Schist (Waiho River). C' shear sense is synthetic to bulk shear in Alpine mylonite zone, whereas c' shear is antithetic.

of the Aspiring Terrane (Fig. 2). This main planar zone occurs on the overturned limb of a kilometre-scale F_3 (Alpine) antiform closing to the SE (Figs. 3 and 5a). Rocks in the main planar zone preserve a strongly laminated S_2 foliation that dips steeply SE. A quartz rodding lineation on S_2 pitches moderately SW and is approximately parallel to the hinges of F_2 isoclines in the zone, suggesting that the lineation is inherited from D_2. The lineation is also subparallel to the hinges of sparse F_3 microfolds of S_2, which have been retained despite the decrenulation process. Thus the rodding lineation may be a composite fabric element combining elements of both the early and Alpine deformations. In planar zones, quartz veins crosscutting S_2 at a high angle were ptygmatically folded during D_3 (Fig. 5c).

West of the main planar zone is a second folded zone consisting of coarse-grained garnet–oligoclase zone rocks. These are referred to as the western folded zone. There, 3–15-mm-thick quartzose segregations parallel to S_2 are folded about S_3 (Fig. 4a). Inclusions in garnet reveal that biotite was stable in S_2 at this deep structural level. Farther west, within 2 km of the Alpine Fault, S_3 becomes overprinted by the late Cenozoic mylonitic fabric (S_m). In Tatare Stream a ~10-m-wide transition zone separates rocks that have a recogniseable Alpine foliation (S_3) from distal mylonitic rocks farther west that contain shear bands and a mylonitic foliation (S_m) that strikes parallel to the Alpine Fault. Distal mylonitic rocks contain mica fish, quartz ribbon grains and conspicuous oblique grain-shape fabrics. S_m is cut by less steeply dipping extensional shear bands (C') to define a C'-type shear band cleavage (Passchier and Trouw, 1996) that is pervasive at a scale of <1 cm throughout the distal mylonite zone. Most shear bands indicate a dextral-reverse sense of shear that is synthetic to the Alpine Fault, but antithetic shear bands are also common, especially at thin-section scale (Figs. 5b and 6f). The antithetic shears include both ductile and (calcite–chlorite-lined) brittle types, implying continued activity during exhumation of the mylonitic rocks through the brittle-ductile transition zone (Holm et al., 1989). Nearer to the Alpine Fault, in Hare Mare Creek, a transition between the distal mylonite zone and the rest of the Alpine mylonites takes place over ~200 m together with an apparent increase in finite strain (Fig. 2). The transition is expressed by decreases in the mean dip of the mylonitic foliation, of the dihedral angle of C'-type shears to that foliation (S), of the thickness of foliation laminae (<1 mm) and of the mean grain-size. Despite intense deformation, stretching lineations are indistinct in mylonite except in quartzose bands, suggesting an oblate bulk finite strain.

5. Exhumed late Cenozoic brittle-ductile transition zone

Glaciated outcrops at Franz Josef Glacier in biotite-zone rocks of the eastern folded zone expose a ~1–2-km-thick zone of brittle-ductile shears at a structural distance of 7 ± 1 km above the Alpine Fault (Fig. 3, A–A′). This zone strikes ~055, dips ~35–55° SE and is approximately parallel to the Alpine Fault. We interpret it as a fossil late Cenozoic brittle-ductile transition zone (BDTZ) that has been exhumed by uplift and erosion on the Alpine Fault. The shears in this zone have a remarkably systematic mean spacing of $\sim 0.5 \pm 0.5$ m (2σ) (Fig. 4d). Because they cross-cut the Alpine foliation (S_3), and are infilled with fibrous fault-surface veins bearing the low temperature assemblage quartz + carbonate + chlorite (Craw, 1997), the shears (S_{bds}) are included with the mylonitic foliation (S_m) as late Cenozoic (D_4) structures. Older quartz-siderite veins are deflected and thinned as they pass though the shear zones (Fig. 4d), where they acquire a shear-related sigmoidal foliation (elongate grain-shape fabric) and a lattice preferred orientation. Finite displacement of the quartz veins across each shear (typically ~5–40 cm) is accommodated by crystal–plastic shear mechanisms across ductile deformation zones that are ~2–10 cm wide. Ductile displacement is most common where the deformed veins are >1 cm thick, whereas thinner veins (and the host psammite matrix) are offset brittlely across 1–2-mm-wide fracture surfaces lining the centre of the shears. The mean ratio of ductile/brittle offset increases downward across the BDTZ as does the width of foliated mylonitic rocks bordering the shears. The shears are remarkable for their uniformity of attitude, spacing and displacement, and for their lack of associated gouge, pseudotachylyte or other fault rocks suggestive of high strain-rates or coseismic brittle-frictional behaviour.

The position of this exhumed BDTZ in the structural pile is consistent with thermochronological data and changes in quartz microstructure as a function of depth in the Alpine Schist. Assuming a maximum temperature of 525 ± 25°C at the base of the mylonite zone (Grapes and Vry, 1999) and a pre-uplift geotherm in the Pacific Plate of ~20°C/km (Kamp, 1997), rocks presently 7 ± 1 km up-section from the Alpine Fault would originally have resided at 385 ± 45°C. This estimate ignores any modifications to late Cenozoic paleoisotherms due to strain. Thermochronological data along the Whataroa transect (Fig. 3, A–A′) place the projected structural position of the BDTZ below the base of the partial annealing zone for zircon fission tracks (T = c. 240–365°C), and above the base of the partial retention zone for Ar-diffusion in white mica (T = c. 410°) (e.g. Tippet and Kamp, 1993; Gallagher et al., 1998; Batt et al., 2000). So far we have identified BDTZ structures in outcrop in the region between the Franz Josef Glacier and Architect Creek, but not outside of this area.

Changes in quartz microstructure with depth reflect a late Cenozoic increment of crystal–plastic deformation below the BDTZ. Quartz in buckled quartz veins above the BDTZ shows foam texture and lacks undulose extinction indicative of static annealing (Fig. 7a). The mean grain-size of these equant-shaped recrystallized grains is ~50–150 μm. Grain boundaries are straight to slightly curved and

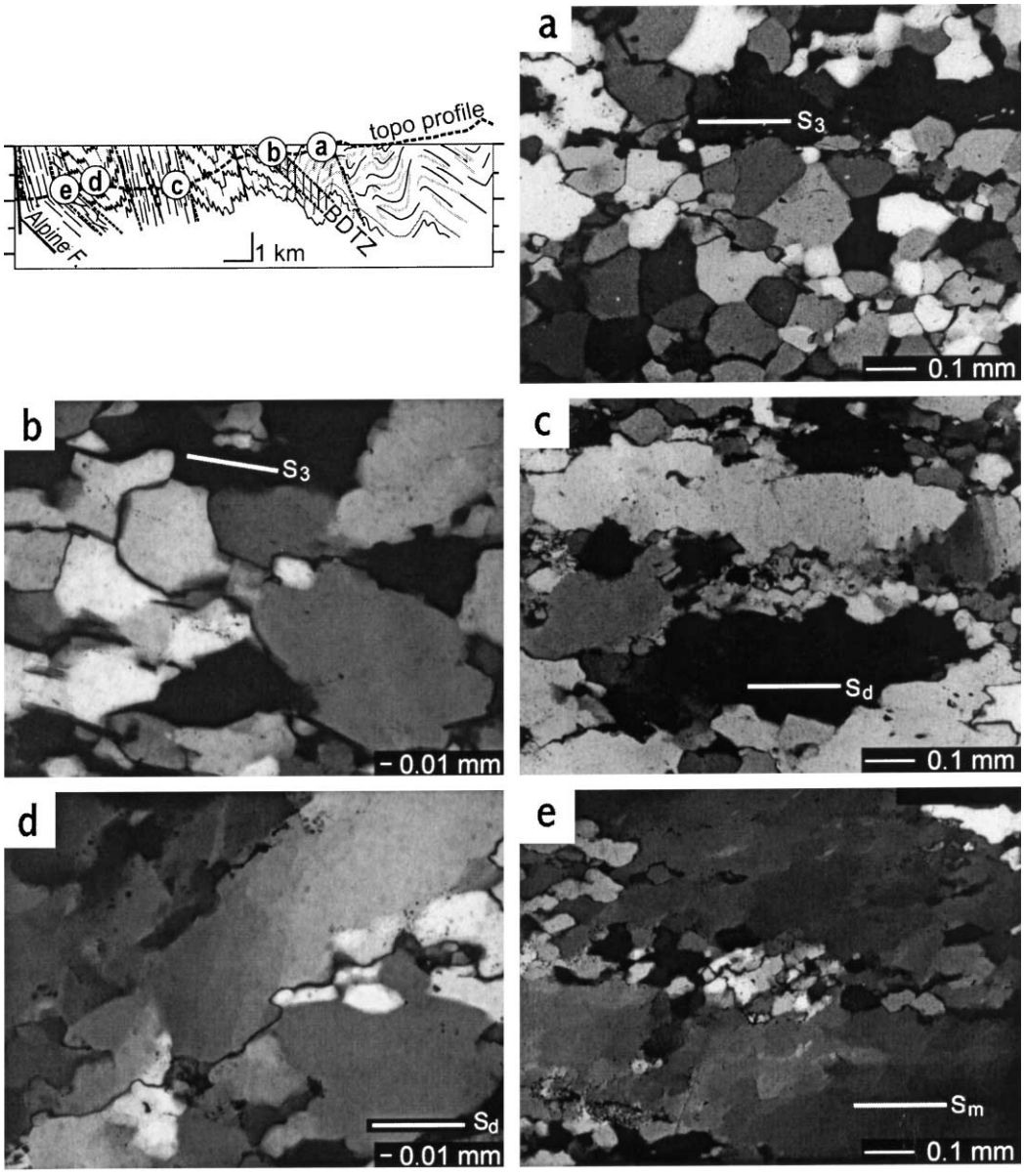

Fig. 7. Photomicrographs (crossed polars) of microstructures in deformed quartz veins at different structural levels of the Franz Josef Glacier transect (see inset). (a) From above the BDTZ at Franz Josef Glacier (biotite zone). Note polygonal-equigranular texture of deformed quartz vein and lack of undulose extinction. (b) From wall rocks of brittle-ductile shears in BDTZ. Note finely dentate grain boundaries and patchy undulose extinction. (c) From main planar zone (garnet zone) below the BDTZ. Note grain–shape fabric, sweeping undulose extinction, deformation bands, dentate grain margins, and recrystallised grains. (d) From lower folded zone near albite-out isograd. Note recrystallised grains, deformation bands, abundant subgrains and obliquity of grain-shape fabric (normal shear sense). (e) From distal mylonite zone. Note core-and-mantle structure, abundant recrystallised grains and subgrains, and oblique grain-shape fabric (reverse shear sense).

smooth. Within the BDTZ at slightly deeper levels, deformed quartz veins retain the polygonal texture, but have acquired patchy undulose extinction and a new grain-shape fabric parallel to the main (S_3) foliation (Fig. 7b). Most grain boundaries are irregular and contain tiny involutions or bulges, indicative of high dislocation densities with recovery by grain-boundary migration. The textures are mostly equigranular, subgrains are rare, and optically resolvable recrystallised grains are absent. Inside ductile shear zones of the BDTZ, deformed vein quartz has an elongate grain-shape fabric and lattice preferred orientation. Fluid inclusion streams along healed microcracks local microfaulting suggest semibrittle deformation.

Below the BDTZ and extending down into the garnet zone, quartz grains in deformed veins retain inherited elements of the originally polygonal microstructure, but are characterised by patchy to sweeping undulose extinction, by abundant deformation lamellae and deformation bands, and by grain boundaries that become increasingly interlobate with depth. An elongate grain-shape fabric is

present and the grain size distribution is no longer equigranular (Fig. 7c). Sparse recrystallised grains are typically 10–30 μm in diameter. In the main planar zone, oblique grain-shape fabrics and 20–100 μm diameter subgrains occur in areas of locally high strain (Fig. 10a). A transition in quartz microstructure occurs in nonmylonitic rocks near the albite-out isograd. There, quartz aggregates in deformed veins become seriate-interlobate in texture and contain a significant fraction of recrystallised grains. Abundant subgrains, deformation bands, core-and-mantle structures, and oblique grain-shape fabrics suggest recovery by dislocation climb and grain-boundary rotation recrystallisation (Fig. 7d). Bulged grain boundaries indicate that grain boundary migration continued to be an important process. Similar microfabrics also typify the distal mylonite zone (Fig. 7e), but the fraction of recrystallised grains is much larger.

The above description of quartz microstructures refers to quartz veins in the Alpine Schist that lie entirely within the nonmylonitic part of the crustal section >2 km from the Alpine Fault, and which have been buckled and/or stretched in the steeply dipping plane of the Alpine foliation (S_3). As we shall see, shear fabrics in these rocks differ in their shear sense from those in the adjacent Alpine mylonites. Hirth and Tullis (1992, 1994) documented quartz microstructures associated with experimental deformation of quartzite, and described transitions between semibrittle flow and several regimes of dislocation creep as a function of increasing temperature or decreasing strain-rate. The progression of quartz microstructures in the Alpine Schist resembles that obtained on quartz aggregates subject to deformation across their experimental brittle-ductile transition. In particular, quartz microstructures in the Alpine Schist just below the BDTZ resemble their lowest temperature regime of dislocation creep (regime I of Hirth and Tullis, 1992), whereas those close to the Alpine Fault strongly resemble their higher temperature regime III; however, the correspondence between their experiments and the Alpine Schist fabrics is not perfect. Microstructures indicative of grain-boundary migration are common throughout the Alpine Schist rocks below the BDTZ, whereas Hirth and Tullis's (1992) experimental study predicts that these should be rare in an intermediate-temperature zone (their regime II), in which recovery occurs primarily by subgrain rotation recrystallisation.

We interpret quartz textures above the BDTZ to have remained annealed during the long interval of crustal residence following the main Alpine metamorphic event (D_3) and to be unaffected by late Cenozoic ductile deformation (D_4). By contrast, quartz veins structurally below the late Cenozoic BDTZ contain grain-shape fabrics and disequilibrium quartz microstructures that were superposed on the older annealed fabrics. We infer that these deeper rocks record an imprint of crystal–plastic deformation that was acquired, and frozen-in, during the current phase of oblique convergence. This imprint took place by constructive reinforcement of the Alpine foliation (S_3), which was ideally predisposed to accommodate a further increment of late Cenozoic transpression, as discussed in the next section.

6. Fabric orientation relative to the Alpine Fault

The Alpine (S_3) foliation in the nonmylonitic part of the Alpine Schist near Franz Josef and Fox Glaciers is near-vertical and strikes ~040 in contrast to the Alpine Fault, which strikes ~050 (Fig. 8a and b). In cross-section, the foliation trajectory pattern is fan-like, with dips decreasing towards the Alpine Fault and approaching parallelism with that structure. At >8 km from the fault, S_3 dips 70–80° NW (Fig. 9a). At ~8 km it steepens through the vertical. Between ~8–4 km from the fault, the dominant foliation dips 70–80° to the SE. Farther west, foliation dips progressively decrease and S_3 dips ~50–60° SE at the edge of the distal mylonite zone. Close to the fault, the mylonitic fabric (S_m) replaces S_3 but the pattern of westwardly decreasing foliation dips persists. The mylonitic foliation shallows to 25–30° adjacent to oblique-thrust strands of the Alpine Fault, such as in Hare Mare Creek (Norris and Cooper, 1997) and other streams near Fox Glacier. In plan view, the strike angle between the dominant foliation and the Alpine Fault is a constant ~10–15° at 4–11 km from the fault (Fig. 9b). At <4 km, however, this horizontal angle tends to narrow towards zero. Although its attitude is locally variable due to post-mylonitic kinking, thrust-duplexing, and gravity-collapse, the mean mylonitic foliation (S_m) is at most only slightly discordant to the Alpine Fault (Sibson et al., 1981; Norris and Cooper, 1997). We interpret the above data to indicate that ductile shear related to the Alpine Fault extends ~3–5 km into the hanging wall of that structure. The mechanism may have involved antithetic slip and forward rotation of the foliation (S_3). Such a bookshelf-like process is mechanically favoured where an anisotropy (S_3) lies in the extensional quadrant of bulk deformation at large angle to the shear plane (e.g. Williams and Price, 1990), and clearly affects biotite laths at the microscopic scale (e.g. Fig. 10b).

The $L_{2\times3}$ intersection is the dominant lineation in the Alpine Schist. Parallel to the hinges of F_3 crenulations and mesoscopic folds, it typically pitches 30–40° SW in the steeply dipping plane of the Alpine foliation (S_3); the older quartz rodding lineation on S_2 is similarly oriented where it is preserved in the planar zones (Fig. 8a and b). A gentle to moderate SW pitch is typical of fold hinges and intersection lineations throughout the Southern Alps (Lillie et al., 1957; Grindley, 1963; Cooper, 1974; Findlay, 1987; Craw et al., 1994). That this $L_{2\times3}$ lineation is approximately parallel to the Alpine Fault is significant. This supports the interpretation that the early foliation's sheet dip is approximately concordant to the SE-dipping Alpine Fault, a relationship that accords with form surface mapping in the

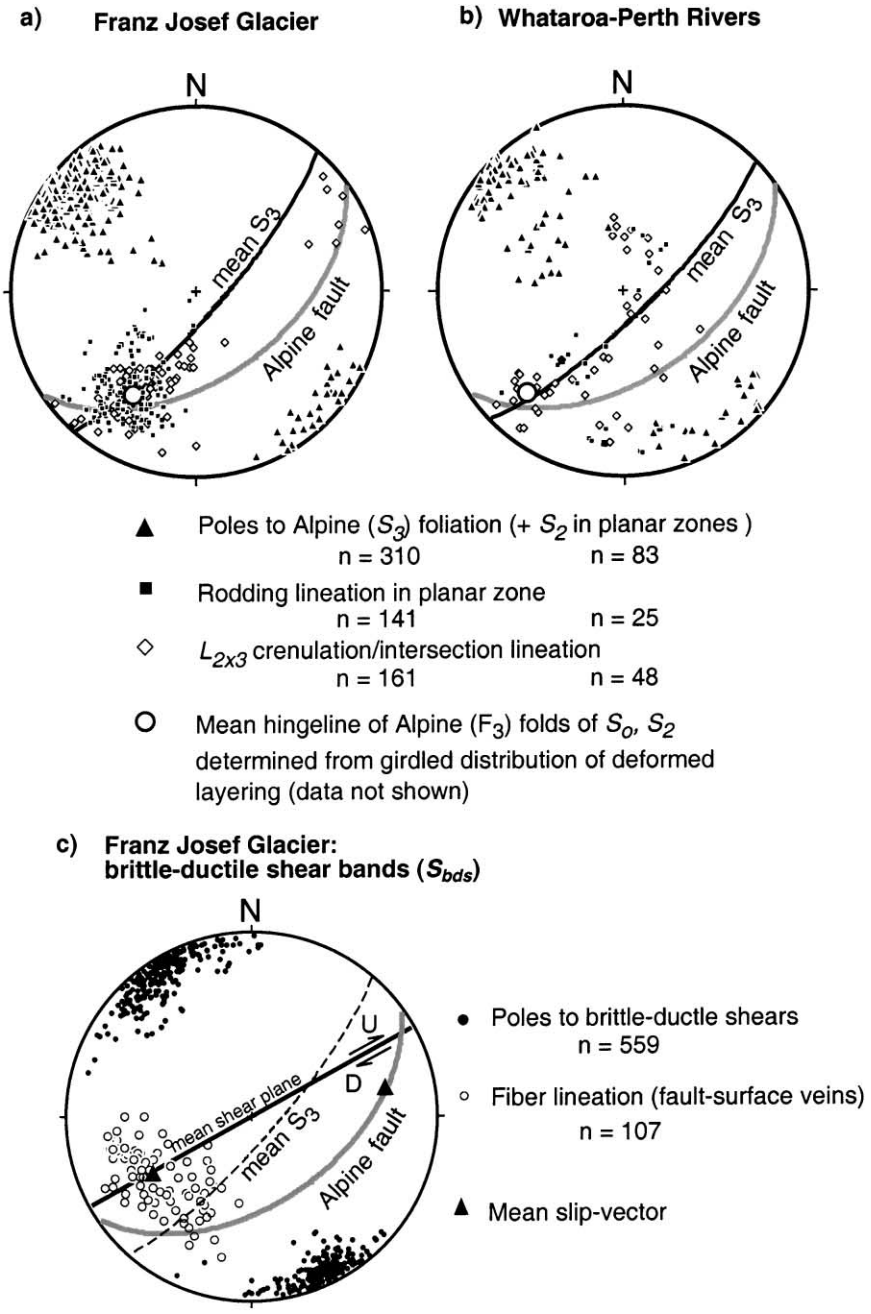

Fig. 8. Lower hemisphere equal-area stereograms showing attitude of selected structures in non-mylonitic Alpine Schist. Estimate of mean Alpine Fault plane is plotted for reference. (a) Alpine foliation (S_3), intersection lineation (L_{2x3}), and mean hingeline of Alpine folds in Franz Josef Glacier transect; (b) same data for Whataroa–Perth Rivers transect; (c) kinematic data for late Cenozoic brittle-ductile shears (S_{bds}) in BDTZ at Franz Josef Glacier. Note how the shear planes strike subparallel to the Alpine Fault, whereas older, Alpine fabric elements trend obliquely to that late Cenozoic structure.

central Southern Alps by us (Fig. 3) and others (e.g. Andrews et al., 1974; Findlay, 1987).

7. Late-stage ductile shear in the Alpine Schist

Brittle-ductile shear zones (S_{bds}) in the BDTZ at Franz Josef Glacier strike, on average, subparallel to the Alpine Fault, and dip within 10° of vertical (Fig. 8c). Fibre lineations on calcite–quartz–chlorite fault surface veins pitch moderately (~40°) to the SW. Older marker layers, such as quartz veins or S_3 foliation laminae, are offset by the shears in a down-to-the-east sense. Their throw is antithetic to the Alpine Fault (Fig. 4d). The same dextral-oblique sense of shear is typical of the Alpine Schist below the exhumed BDTZ. Rather than being confined to discrete

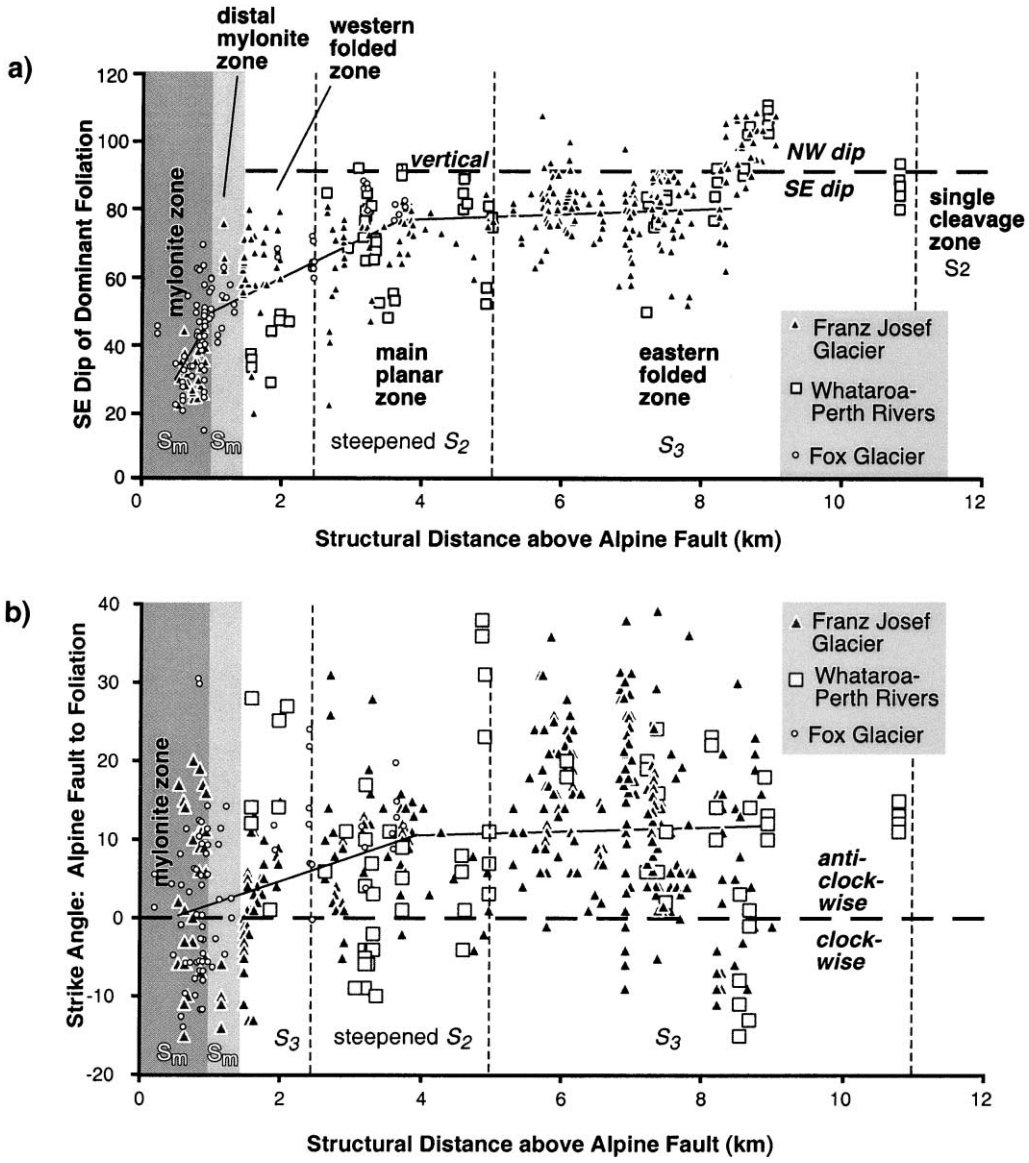

Fig. 9. Scatter plots showing changing dip and strike of foliations in the Alpine Schist as a function of structural distance orthogonal to the Alpine Fault. (a) dip angle of the dominant foliation (S_3 in folded zones, S_2 in planar zones, mylonitic foliation (S_m) in mylonite and distal mylonite zones); (b) horizontal angle between strike of dominant foliation and strike of Alpine Fault. Fine lines show inferred mean trends. Note apparent kinks in both data sets at ~4 km from the Alpine Fault. The distance of structural data points from the Alpine Fault plane were calculated in 3D by vector algebra from map coordinates and elevations stored in a G.I.S. database. The calculation assumes that the mean trace of the Alpine Fault is as shown in Fig. 2, and that the fault dips 50° SE. Changing these input values would not alter the essential spatial trends on the plots. Data from Fox Glacier area is from Wightman (2000).

shear zones, however, this deeper-level shear is widely distributed, and pervades the rocks down to the scale of a thin-section. This downward transition in behaviour is exposed on the eastern wall of Franz Josef Glacier.

Microstructures indicate that ductile deformation at deep levels of the Alpine Schist was noncoaxial. Earlier analyses of shear sense in the Alpine Schist have focused on the Alpine mylonite zone, which has dextral-reverse shear fabrics synthetic to slip on the Alpine Fault (e.g. Norris and Cooper, 1995). Our 20 thin-sections of the mylonitic rocks also contained abundant evidence for dextral-reverse shear, but microstructures near the eastern edge of the distal mylonite zone commonly record conflicting shear sense indicators in a single slide, including complex strain shadows. We believe that these reflect superposition of dextral-reverse shear of the mylonitic fabrics across older, non-mylonitic fabrics that are dextral-normal. Quartz *c*-axis lattice preferred orientation data across the transition supports this reversal in shear sense (Ilg and Little, 1999).

In the nonmylonitic rocks of the Alpine Schist, microstructural evidence of noncoaxial ductile deformation was distinct but less obvious than in the highly sheared rocks of the Alpine mylonite zone. Asymmetric quartz grain-shape

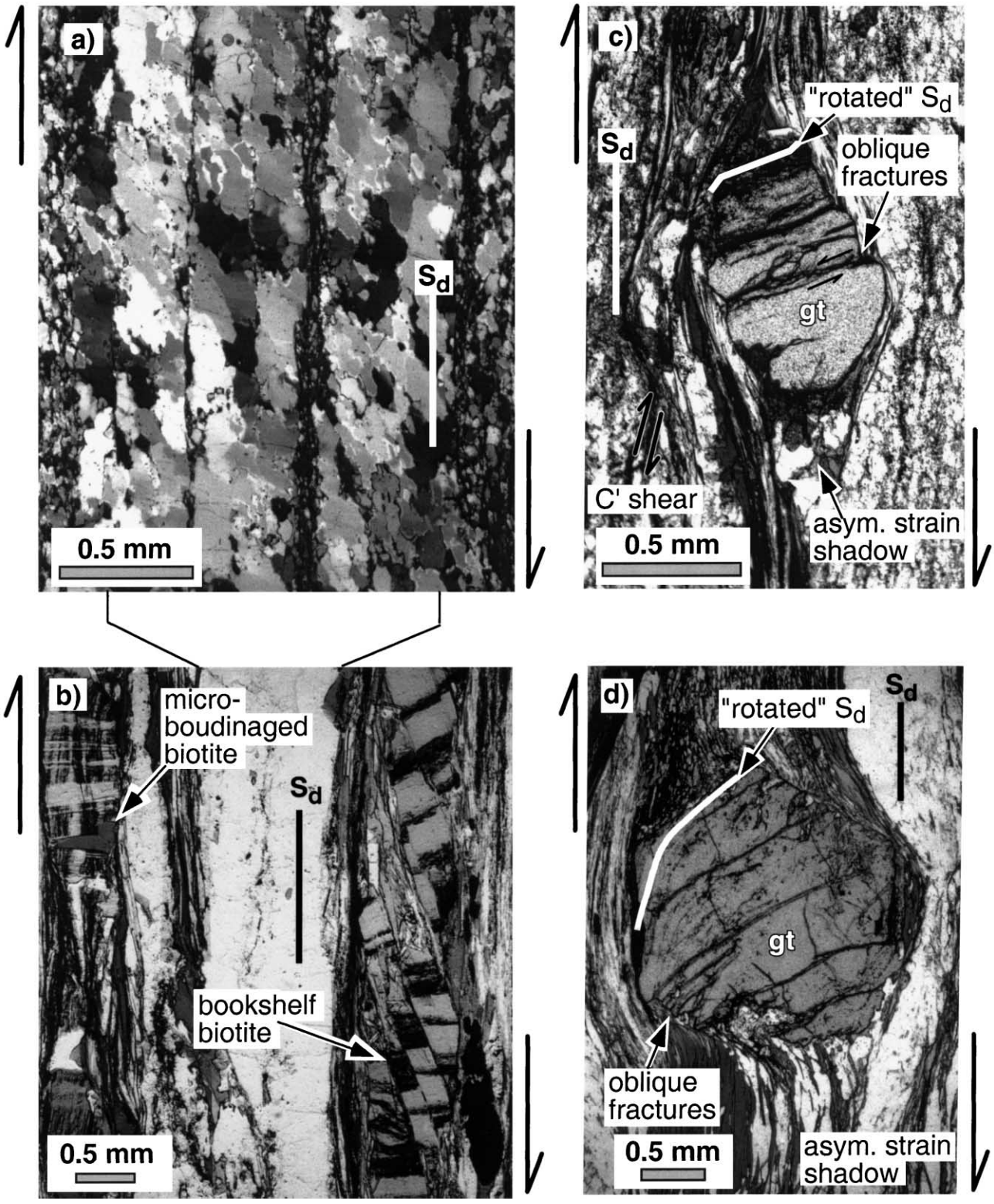

Fig. 10. Photomicrographs of microstructures indicative of shear sense in deeper, non-mylonitic parts of the Alpine Schist (plain light unless otherwise noted). Foliation is steeply dipping and all thin sections are oriented with west on the left and east on the right. 'bio' and 'gt' refer to biotite and garnet. (a) Oblique grain shape fabric in quartz lamination (lower folded and garnet zones). Crossed polars. (b) Enlarged view of same thin section, showing bookshelf sliding (right-hand side) and microboudinage (upper left-hand corner) of disaggregated biotite grains. (c) and (d) Garnets with asymmetric strain shadows, inclusion trails suggesting forward rotation of garnet relative to the foliation trace, and oblique extension fractures. The garnet in (c) is from the lower folded zone on the NW verging limb of an Alpine fold. At least one of its oblique fractures has undergone antithetic slip suggesting forward rotation of bookshelf fragments. The garnet in (d) is from the SE verging limb of the Robert's Point antiform (main planar zone). Despite (c) and (d) occurring on oppositely verging fold limbs, the sense of shear in both is down to the east.

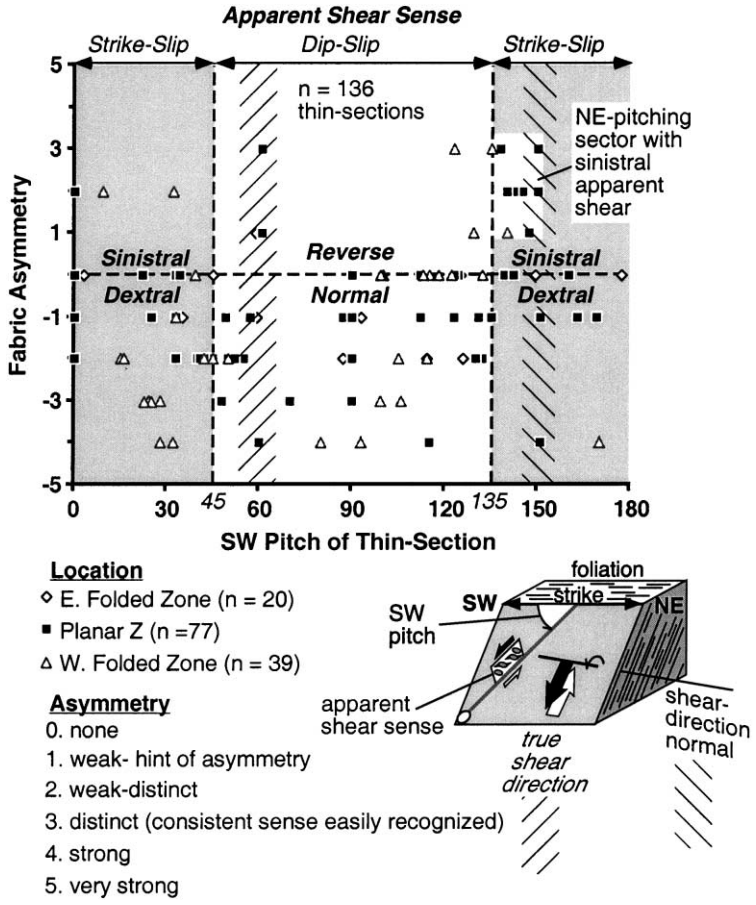

Fig. 11. Summary of apparent slip sense and shear fabric intensity in the 136 oriented thin-sections of nonmylonitic biotite-zone and higher-grade Alpine Schist from the Franz Josef Glacier and Whataroa River areas (data for the Alpine mylonite zone and distal mylonite zone are excluded). At least two perpendicular thin-sections were cut orthogonal to foliation in each of 220 samples. Only data pertaining to those samples that yielded shear-sense information on at least one thin-section plane is plotted. Pitch in the Alpine foliation plane specifies the orientation of each thin-section. Where a shear sense could be inferred from microstructures in a thin section, this sense is described either by its apparent sense of strike-slip (for sections pitching $<45°$; +ve is sinistral, −ve dextral), or by its apparent sense of dip-slip (for sections pitching $>45°$; +ve is reverse, −ve normal). A qualitative scale of degree of fabric intensity is plotted along the vertical axis. The cross-hatched pitches are our interpretation of the mean shear direction and its normal. The Table (on-line data archive) gives a detailed description of the petrographic data used to construct this plot, as well as a list of shear sense criteria applied to 20 additional samples of mylonitic rocks (chiefly dextral-reverse).

fabrics (Means, 1981; Lister and Snoke, 1984) are the most common index of shear-sense, occurring in most samples with quartz-rich laminae (Fig. 10a). Slightly less common are asymmetric strain shadows adjacent to garnet, ilmenite, and biotite grains (Fig. 5c). Most garnet grains are split by intragranular extension cracks. In thin-section, the traces of these cracks commonly make an angle of 60–80° to the foliation. This obliquity suggests a discordance between the instantaneous and finite directions of stretching that is indicative of shear sense (Fig. 10c and d). This sense is always accordant with other indicators in the same sample. Many equant garnet grains contain inclusion trails that can be traced outward into the external foliation. The orientation of the internal foliation and shape of partially overgrown strain shadows show a consistent sense of rotation of the garnet relative to the external foliation throughout the slide. C'-type (extensional) shear bands can also be used to infer the bulk shear sense in some nonmylonitic rocks of the Alpine Schist, but may be unreliable due to the conjugate nature of shear bands associated with foliation boudinage (Figs. 5b and 6f). Asymmetric muscovite or biotite fish are typically present in mylonites (Fig. 5b). Finally, Holcombe and Little (2001) used inclusion trail geometries in biotite laths from the main planar zone at Franz Josef Glacier to document asymmetric patterns of rigid-body rotation due to a down-to-the-east sense of shear.

In an attempt to constrain the direction of shear, we cut two or more thin-sections perpendicular to the foliation for each of 220 samples of nonmylonitic, biotite-bearing Alpine Schist (Table on-line data archive[1]). The sections were cut parallel and perpendicular to foliation strike; or,

[1] See "Electronic Supplements" on this journal's homepage http://www.elsevier.com.locate.jstrugeo

alternatively, parallel and perpendicular to the intersection lineation ($L_{2\times3}$). We qualitatively ranked degree of fabric asymmetry or apparent shear intensity in each thin-section on a scale between 0 and 5, with 0 indicating no evidence for shear and 5 indicating intense shear fabrics (Fig. 11). Commonly, asymmetric fabrics indicative of ductile shear were apparent on only one of the two foliation-orthogonal thin-sections. About ~40% of the nonmylonitic samples, including most of those above the BDTZ, are characterised by orthorhombic fabrics on both sections, consistent with no shear.

Shear sense indicators in nonmylonitic rocks reveal that oblique top-down-to-the east shear pervades the main planar zone and the two folded zones of both transects (arrows in Fig. 3). This sense of shear occurs on both limbs of Alpine fold structures (compare Fig. 10c and d), and is representative of bulk deformation throughout the Alpine Schist. The sense of strike-slip is synthetic to the Alpine Fault, whereas the sense of dip-slip is antithetic. Shear on horizontal sections is chiefly dextral; typically it is much less intense than that on down-dip sections. The overall relationship between fabric asymmetry and thin-section pitch can be used to infer the mean direction of shear. In Fig. 11, note the diffuse trend of increasing fabric intensity towards maxima at SW pitch angles of between 30 and 80°. Importantly, thin-sections pitching SW at 135–150° have a sinistral apparent shear-sense, whereas those pitching >150° are apparently dextral. We interpret this transition to mark the orientation of the shear-direction normal. The mean shear direction is thus inferred to pitch SW at ~60° SW, somewhat steeper than the $L_{2\times3}$ intersection lineation.

Ductile flow was probably transpressive rather than a simple shear. Holcombe and Little (2001) documented patterns of rigid-body rotation of biotite laths relative to the Alpine foliation, compiling plots of the angle between the internal and external foliations in these laths versus the angle between their long-axes and the external foliation. Applying the equations of Ghosh and Ramberg (1987) for rotation of rigid inclusions in a general flow, they inferred a dip-slip (down-to-the east) shear strain of ~0.6, and a sectional kinematic vorticity number (Wk) of 0.2–0.3 for nonmylonitic Alpine Schist. Back-rotated biotite laths are common, indicating a significant irrotational component to the cumulative deformation since growth of these laths (Fig. 6e). Other evidence for non-simple shear in the Alpine Schist includes the 60–80° dihedral angle that garnet extension fractures typically make to the Alpine foliation in sheared rocks of the Alpine Schist. In simple shear the instantaneous direction of maximum shortening rate is ~45° to the shear plane. For a plane deformation a 60–80° angle would correspond to a kinematic vorticity number of 0.6, but this would be an overestimate in the more likely case of 3D deformation (see Fig. 2 of Tikoff and Fossen, 1995). Transpressive flow is implied by lattice preferred orientation patterns for quartz *c*-axes in both mylonitic and nonmylonitic parts in the Alpine Schist; commonly these have a monoclinic symmetry departing only slightly from orthorhombic (Ilg and Little, 1999). Extensional shear bands occur in conjugate sets in both nonmylonitic and mylonitic parts of the Alpine Schist. These accommodate an extension of the shear plane indicative of a transpressive type of flow (e.g. Platt and Vissars, 1980; Tikoff and Fossen, 1999).

8. Discussion and conclusions

8.1. Superposition of neotectonic strain by reinforcement of pre-existing fabrics

The onset of convergence between the Pacific and Australian plates is inferred from seafloor spreading data to have begun at ~6.4 Ma (Walcott, 1998). Although the age of the Barrovian Alpine metamorphism is still uncertain, including the likelihood diachronous phases of mineral growth, available geochronological data suggests a dominant Late Cretaceous to possibly Miocene age (e.g. Chamberlain et al., 1995; Batt et al., 2000; Vry et al., 2001). Thus, the synmetamorphic Alpine foliation (our S_3) is almost certainly an inherited fabric relative to the late Cenozoic oblique convergence that has caused uplift of the Southern Alps. Today, this fabric crops out in a 10–30-km-wide zone bordering to the Alpine Fault, and its NNE-striking foliation and folds have an en échelon arrangement to that structure (Fig. 2). At ~6.4 Ma, these fabrics would have been 50–80 km farther east of that structure where they would have resided at ~30 km depth.

Thermochronological and thermobarometric data indicate that Alpine Schist rocks outcropping near Franz Josef Glacier resided in the middle crust at temperatures of ≧500°C as recently as 3 Ma (e.g. Chamberlain et al., 1995). An important conclusion of this study is that outside of the narrow mylonite zone, ductile deformation related to the current phase of oblique convergence did not result in pervasive superposition of a new foliation on the rocks, but rather in constructive reinforcement of the pre-existing Alpine fabric. Orthogonal to the geodetic direction of maximum shortening rate, this foliation was ideally oriented to accommodate an additional neotectonic strain. Microstructurally, the overprint caused boudinage and bookshelf tiling of biotite laths, elongation of strain shadows, and tightening or decrenulation of microfolds. Structural geologists often attribute successive generations of foliations to an equivalent number of deformation phases. This approach overlooks the potential for a foliation to lie in the extensional quadrant of a later incremental strain, a situation that will result in stretching and intensification of the original fabric rather than its crenulation or transposition. Based on careful examination of a recently exhumed crustal section, our work may serve as a caution to those working in ancient terranes.

The rheological behavior of a foliation once it has been

imprinted into a rock is a classical problem in structural geology (e.g. Williams, 1976). Our data strongly suggests that during its ramping and uplift during the past several million years, the Alpine foliation either behaved as a passive marker attached to material points (e.g. Hobbs et al., 1982; Wright and Henderson, 1992), or as an active surface tracking towards (but perhaps never coinciding with) the *XY* principal plane of finite strain (Ramsay, 1967; Treagus and Treagus, 1981; Luneburg and Lebit, 1998). At present, we cannot distinguish between these two alternatives. Both involve 'reworking' of a pre-existing fabric, a process that we suspect is common in the deeply exhumed parts of many other active orogens.

Foliation reinforcement has occurred at least three times during the history of the Alpine Schist. Our work has shown that the planar zones in the Alpine Schist represent fold limbs where the early foliation (S_2) has been steepened into subparallelism with the younger Alpine fabric (S_3). S_2 in these zones was constructively reinforced during D_3 causing its laminations to be additionally thinned and stretched (e.g. Fig. 4c). Still more layer-parallel stretching accumulated during the late Cenozoic (D_4), leading to an almost complete decrenulation of microfolds in these planar zones. A final reinforcement episode took place when the mylonitic deformation was overprinted across older Alpine ($=D_{3+4}$) fabrics in the narrow zone bordering the Alpine Fault. Both fabrics contain foliations that dip moderately SE, and the strikes of these differ by $<10°$. Thus the Alpine foliation is in the extensional quadrant of the mylonitic strain. The older foliation occurs as part of a fabric continuum into the mylonite zone, and the transition between S_3 and S_m is gradational (Fig. 6f). In the mylonite zone, D_3 microfolds are preserved as folded inclusion-trail remnants inside garnet porphyroclasts, but have otherwise been completely removed or decrenulated from the mylonitic fabric of the external matrix.

8.2. Late Cenozoic increment of ductile strain in the Alpine Schist

GPS data confirms that oblique convergence in the central South Island of New Zealand is today accommodated across an ~150-km-wide region of distributed transpressive strain, and seismic reflection data has imaged the ~45° dipping crustal ramp along which the upper part of the Pacific Plate is being uplifted and exhumed. How do we know that late (D_4) increments of ductile strain imprinted into the Alpine foliation outside of the mylonite zone are late Cenozoic in age? In the central Southern Alps reset fission-track ages of apatite and zircon are <1 Ma, and $^{40}Ar/^{39}Ar$ and K/Ar ages of biotite, muscovite and hornblende are generally <1, <3 and <5 Ma, respectively (Tippet and Kamp, 1993; Chamberlain et al., 1995; Batt et al., 2000). These ages record cooling and exhumation of the crustal section during Pliocene and younger uplift along the Alpine Fault. Although these data suggest that the high-grade part

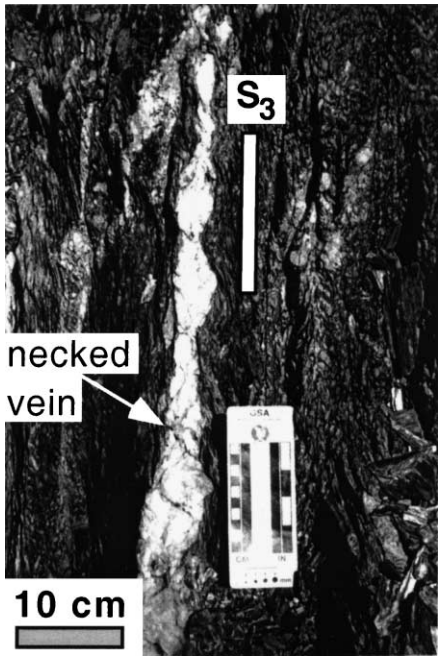

Fig. 12. Photograph showing ductile necking of quartz–muscovite–chlorite vein of probable late Cenozoic age in the Alpine foliation near the garnet-in isograd at Baumann Glacier on the west side of Franz Josef Glacier Valley.

of the schist has been exhumed from >500°C during the last few million years, well within the regime of ductile deformation for crustal rocks, they do not constrain the age of any strain increment contributing to the rock's deformational fabric. The occurrence of foliated, ductilely deformed ~68 Ma pegmatite dikes in the Alpine Schist north of Haast suggests a Cenozoic contribution to ductile fabric development in the Alpine Schist (Chamberlain et al., 1995; Batt, 1997). Similarly, at Franz Josef Glacier, drusy-textured quartz–muscovite–chlorite ± adularia veins emplaced subparallel to S_3 have pinch-and-swell structures indicative of ductile necking (Fig. 12). The coarse quartz grains contain abundant microstructures indicative of crystal plasticity, including subgrains, deformation bands, undulose extinction, and lattice preferred orientation. Fluid inclusion studies on other similar veins by Craw (1997) and Cox et al. (1997) indicate fluid trapping during hydrothermal boiling at temperatures of 240–350°C and at depths of 0.5–2 km, probably during late Cenozoic unroofing. Adularia from a vein near the Almer Glacier yielded a maximum $^{40}Ar–^{39}Ar$ age of ~880 ky (Teagle et al., 1998). The necking implies a significant late Cenozoic contribution to ductile strain.

Identification of an exhumed late Cenozoic BDTZ at ~7 ± 1 km above the Alpine Fault at Franz Josef Glacier is a key piece of evidence indicative of a late Cenozoic deformation age. There, brittle-ductile shears in the BDTZ strike subparallel to the Alpine Fault and the zone as a whole dips subparallel to that structure. The shears have a dextral-oblique sense of strike-slip, are infilled by low-temperature vein assemblages, and crosscut all other deformational

fabrics except for the above-mentioned fissure-filling veins bearing adularia. Quartz–carbonate–chlorite veins infill the vertical shears, recording upward leakage of fluids into the brittle crust, probably from an underlying zone of overpressured metamorphic fluids. Such a zone near the Alpine Fault has recently been imaged geophysically using both seismic and magnetelluric data (Wannamaker et al., 2001; Stern et al., 2001).

The position of the BDTZ in the crustal column was probably controlled by the late Cenozoic thermal structure in the Alpine Schist at some point during its uplift and exhumation history, especially at the location of 300–400°C isotherms. Changes in quartz microstructure that take place across the BDTZ, including the addition of a quartz grain-shape fabric below it, indicate that the last increment of ductile strain is late Cenozoic.

Another key observation is that the late Cenozoic brittle-ductile shears (S_{bds}) near Franz Josef Glacier merge downward into pervasively back-sheared garnet-zone rocks below the BDTZ. This shear, dextral-oblique and east-side-down, overprints the limbs and hinges of older D_3 (Alpine) folds, and is not a product of flexural flow. Importantly, this backshearing makes sense in the current geodynamical context, as it accommodates tilting of the delaminated schists onto the SE dipping ramp of the Alpine Fault (Fig. 13).

Late Cenozoic mylonitic fabrics record a metamorphic history and microstructural sequence that is similar to that of adjacent nonmylonitic fabrics. This suggests a continuum between the two, and thus at least a partial overlapping of their ages. In both zones, antitaxial strain shadows are syntectonically infilled by plagioclase + biotite + muscovite + quartz in their distal, earlier parts; and chlorite + quartz in their proximal, youngest parts. Both the mylonitic and nonmylonitic fabrics have strongly oblate quartz grain-shape fabrics, chocolate-tablet boudinage in 3D, and indistinct or absent elongation lineations in hand sample; and conjugate arrays of extensional shear bands define foliation boudins in both zones (Holm et al., 1989; Little et al., 2002).

Finally, a late Cenozoic component to Alpine folding is suggested by the NE-trend of the tight folds near the Alpine Fault in contrast to the en échelon, NNE-trending disposition of more distant folds, which are less tightly appressed. The crystalline footwall of the Alpine Fault is probably behaving like a rigid indentor (e.g. Koons, 1992), and some fold tightening seems to have occurred during the several m.y. that the presently exposed rocks have been juxtaposed against the Alpine Fault.

8.3. Significance and extent of the Alpine fabric in the Southern Alps orogen

Reflecting earlier usage, we call the steeply dipping foliation in the Alpine Schist at Franz Josef Glacier and Whataroa River the Alpine (S_3) fabric. Characterised by a NNE-strike, near vertical dip, crenulations and kilometre-scale folds with SW-pitching hinges, and distinctive garnet and biotite porphyroblasts, this foliation appears to extend laterally for at least 400 km along the upturned and deeply exhumed western edge of the Pacific Plate. In studies embracing most of the central Southern Alps, Lillie et al. (1957), Gunn (1960), Grindley (1963), Andrews et al. (1974), Grapes (1995), Cooper (1974), Findlay and Sporli (1984), Findlay (1987), and Craw et al. (1994) all describe a steeply dipping crenulation fabric. While acknowledging the pitfalls of fabric correlation, we believe that these authors refer to a single, laterally continuous fabric in the Alpine Schist that developed synchronously with its high-temperature metamorphism. This belief is founded on our own reconnaissance data between Architect Creek and the Ahaura River, a distance of ~250 km, and on our reading of published accounts, especially those documenting textural relationships between the foliation and metamorphic minerals. It also echoes the earlier suggestions of Grindley (1963) and Findlay (1987).

The relationship of the regionally extensive Alpine (S_3) foliation to the late Cenozoic transpression phase is controversial. Some have proposed that the crenulated Alpine fabric (our S_3) developed in a wide zone of distributed dextral wrench deformation between the Pacific and Australian plates approximately coevally with early Miocene inception of the Alpine Fault as a dextral-slip transform (e.g. Findlay, 1987). If so, our microstructural data indicates that the isograd-forming high-temperature metamorphism in the Alpine Schist would also have to be Miocene. One or more Cenozoic phases of mineral growth or exhumation are supported by recent Sm–Nd dating of zoned garnet (Vry et al., 2001), and by K/Ar and Ar–Ar mica ages in rocks to the south of the central Alpine region of highest uplift rate (Batt et al., 2000). The ~15° obliquity of the synmetamorphic Alpine foliation to the Alpine Fault is thus in part an inherited structure. East of the Main Divide, kilometre-scale folds of bedding occur throughout in prehnite–pumpellyite facies rocks of the Torlesse Terrane and are probably Mesozoic in age; these structures that have upright axial planes that strike N to NNE, locally with a slaty cleavage (Lillie and Gunn, 1964; Sporli and Lillie, 1974; Findlay and Sporli, 1984). If folds like these were swept westward into deep structural levels of the obliquely convergent Southern Alps orogen during the late Cenozoic, they could have absorbed the neotectonic strain increment by tightening and clockwise rotation of the folds along with reinforcement of their foliation (Fig. 13b and c).

8.4. Implications for processes of oblique plate convergence

Most workers agree on the crustal-scale kinematics of oblique convergence between the Australian and Pacific Plates (Wellman, 1979; Norris et al., 1990; Koons, 1992). Delaminating at an inferred depth of ~30 km in the central Southern Alps, the upper part of the Pacific Plate crust is

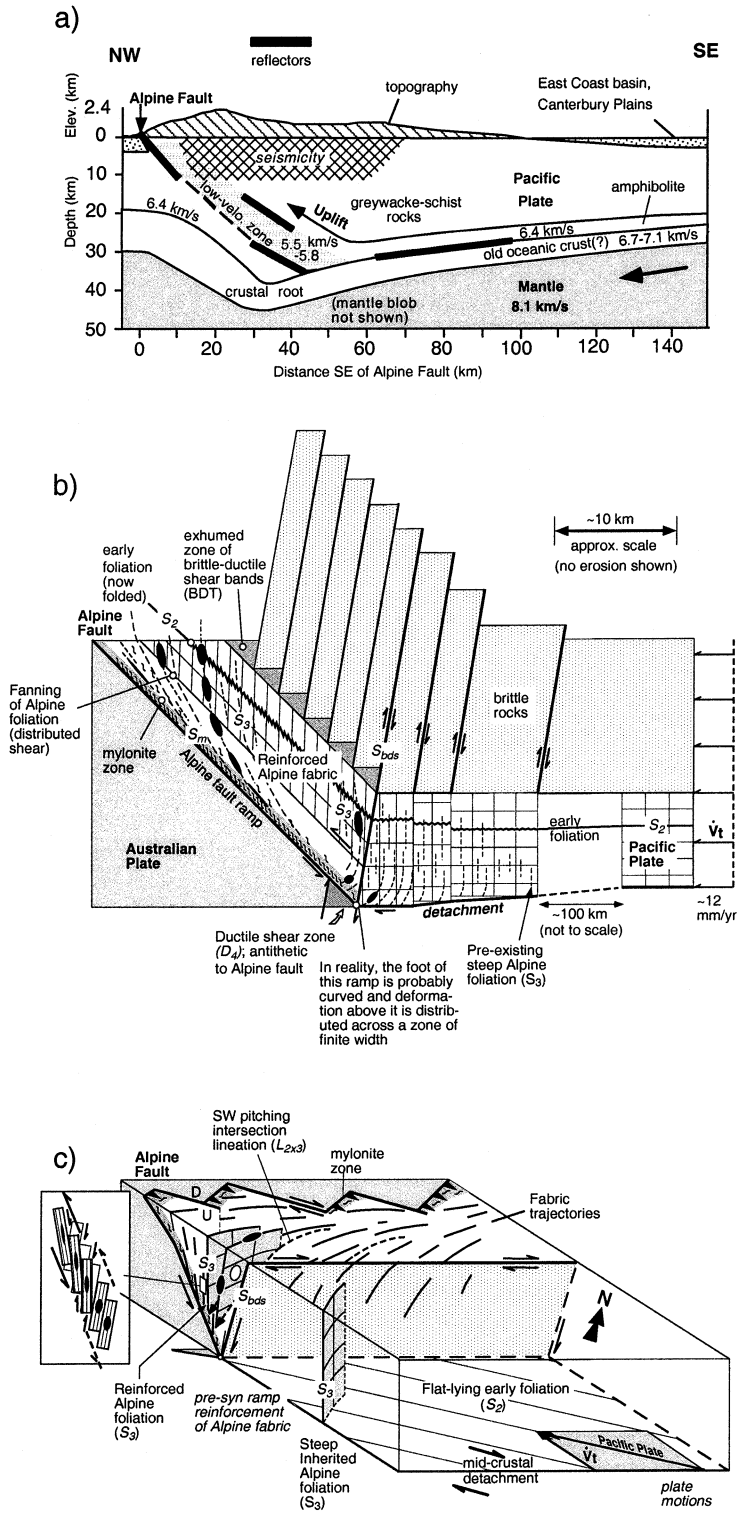

Fig. 13. Geodynamical interpretation of late Cenozoic deformation in the Alpine Schist in relation to the Alpine Fault and South Island plate boundary zone. (a) Preliminary interpretation of crustal structure of SIGHT seismic transect across the central South Island, Mt Cook–Copeland Valley region, New Zealand (from Stern et al., 1997; Davey et al., 1998; Kleffman et al., 1998). (b) Cartoon showing inferred cross-sectional relationship of Alpine Schist fabrics to late Cenozoic oblique convergence between the Pacific and Australian Plates, central Southern Alps. V_t is the convergent component of plate motion. (c) Schematic block diagram showing inferred relationships between Alpine Schist fabrics and Southern Alps orogen.

displaced westward and ramped upward along the oblique-slip Alpine Fault, where it is exhumed by rapid erosion along the western flank of the Southern Alps (Fig. 13a). At greater depths, P-wave delays of teleseismic waves suggests that Pacific Plate's upper mantle has been deformed by 'pure shear' into a blob, >100 km thick, beneath the orogen's ~45-km-thick crustal root (Molnar et al., 1999).

Pacific Plate rocks on the hanging wall of the Alpine Fault preserve successively older ductile fabrics towards the structural top of the tilted crustal section. The early foliation (S_2) and the BDTZ both dip, on average, moderately to the SE, subparallel to the Alpine Fault (Fig. 13b). This observation supports the view that the Pacific Plate is delaminating along a midcrustal detachment, with the upper part of its crust ramping upward along the Alpine Fault. S_2 is inferred to be approximately flat-lying in the untilted region to the east of the crustal ramp (Fig. 13c). The early foliation may be broadly correlative to the flat-lying (albeit folded) Jurassic foliation that pervades deeper levels of the domal Otago Schist, a high-strain transposition fabric of similar appearance and low (mostly chlorite zone) metamorphic grade as S_2 in the Southern Alps (e.g. Mortimer, 1993).

The antithetic shear occurring as distributed deformation at deep levels of the Alpine Schist and as discrete brittle-ductile offsets at higher levels in the fossil BDTZ can be understood as a geodynamical response to displacement of the delaminated Pacific Plate onto the oblique footwall ramp of the Alpine Fault, a process that requires bending and rotation of the upper crust (Fig. 13b). Foreshadowed by Wellman (1979), the model is supported by the systematically spaced nature of brittle-ductile shear zones in the BDTZ, which may have been activated sequentially like the stairs of an escalator. Walcott (1998) inferred a flexural-flow style of crustal bending for the Pacific Plate; however, the dominant planar anisotropy in the Alpine Schist is vertical, not parallel to the Alpine Fault, and the sense of shear we have documented in the Alpine Schist is opposite to that expectable for flexural-slip. The shear sense was dextral-oblique, with a mean slip vector pitching SW at ~60°. Holcombe and Little's (2001) down-to-the-east shear strain estimate of ~0.6 in garnet-zone rocks predicts that originally horizontal markers would undergo a bulk rotation of 32° as they were displaced onto the Alpine Fault ramp. This compares favourably with the 50–20° dip of seismic reflectors correlated with the Alpine Fault plane at depths of 7–35 km (Kleffman et al., 1998; D. Okaya, pers. Commun., 2000). Microfabrics indicate a zone-thinning (transpressive) type of finite deformation rather than simple shear.

Dextral-reverse shear near the base of the Pacific Plate probably accumulated later when already-tilted rocks were translated up the Alpine Fault towards the erosion surface. Changes in foliation attitude (S_3 and S_m) across the Alpine Schist define a fan-like trajectory pattern. The zone of distributed ductile shear related to the Alpine Fault includes not only the 1–2-km-thick mylonite zone, but extends 2–3 km upward into the nonmylonitic section. The mean dip of the Alpine foliation (S_3) rotates ~22° in proximity to the fault (Fig. 9). Such rotation of a passive marker in a simple shear zone would require a bulk shear strain of ~1.0–2.0. The actual deformation, however, may be more complex, involving a bookshelf-like rotation of steep foliation planes (Fig. 13c, inset).

Acknowledgements

This work was funded by grants from the Science Faculty, Victoria University of Wellington. Constructive reviews by Scott Johnson and Simon Cox and editorial suggestions by Richard Norris improved this paper. Discussions with, R.H. Grapes, J.K. Vry, T.A. Stern, N. Mortimer, and E. Palmer were also beneficial. Simon Cox (Institute of Geological and Nuclear Sciences) provided some helicopter and field support and shared his unpublished mapping and knowledge about the geology of the central Southern Alps. R. Wightman contributed data to Fig. 9. S. Bush prepared hundreds of oriented thin-sections.

References

Adams, C.J.D., 1979. The age and origin of the Southern Alps. Royal Society of New Zealand Bulletin 18, 73–77.

Adams, C.J., 1981. Uplift rates and thermal structure in the Alpine Fault zone and Alpine schists, Southern Alps, New Zealand. Geological Society of London Special Publication 9, 211–212.

Andrews, P.B., Bishop, D.G., Bradshaw, J.D., Warren, G., 1974. Geology of the Lord Range, central Southern Alps, New Zealand. New Zealand Journal of Geology and Geophysics 17, 271–299.

Batt, G.E., 1997. The crustal dynamics and tectonic evolution of the Southern Alps, New Zealand: insights from new geochronological data and fully coupled thermo-dynamical finite element modeling. Ph.D. thesis, Australian National University.

Batt, G.E., Braun, J., Kohn, B.P., McDougall, I., 2000. Thermochronological analysis of the dynamics of the Southern Alps, New Zealand. Geological Society of America Bulletin 112, 250–266.

Beaumont, C., Kamp, P.J.J., Hamilton, J., Fullsack, P., 1996. The continental collision zone, South Island, New Zealand: comparison of geodynamical models and observations. Journal of Geophysical Research 101, 333–3359.

Beavan, J., Moore, M., Pearson, C., Henderson, M., Parsons, B., Blick, G., Bourne, S., England, P., Walcott, R.I., Darby, D., Hodgkinson, K., 1999. Crustal deformation during 1994–1998 due to oblique continental collision in the central Southern Alps, New Zealand, and implications for seismic potential of the Alpine Fault. Journal of Geophysical Research 104 (B11), 25,233–25,255.

Bishop, D.G., 1972. Progressive metamorphism from prehnite–pumpellyite to greenschist facies in the Dansey Pass area, Otago, New Zealand. Geological Society of America Bulletin 83, 3177–3198.

Braun, J., Beaumont, C., 1995. Three-dimensional numerical experiments of strain partitioning at oblique plate boundaries: implications for contrasting tectonic styles in the southern Coast Ranges, California, and central South Island, New Zealand. Journal of Geophysical Research 100 (B9), 18,059–18,074.

Bull, W.B., Cooper, A.F., 1986. Uplifted marine terraces along the Alpine Fault, New Zealand. Science 234, 1225–1228.

Chamberlain, C.P., Zeitler, P.K., Cooper, A.F., 1995. Geochronologic

constraints of the uplift and metamorphism along the Alpine Fault, South Island, New Zealand. New Zealand Journal of Geology and Geophysics 38, 515–523.

Cooper, A.F., 1974. Multiphase deformation and its relationship to metamorphic recrystallization at Haast River, South Westland, New Zealand. New Zealand Journal of Geology and Geophysics 17, 855–880.

Cooper, A.F., 1980. Retrograde alteration of chromian kyanite in metachert and amphibolite whiteschist from the Southern Alps, New Zealand. Contributions to Mineralogy and Petrology 75, 153–164.

Cox, S.C., Findlay, R.H., 1995. The Main Divide Fault Zone and its role in the formation of the Southern Alps. New Zealand Journal of Geology and Geophysics 38, 489–499.

Cox, S.C., Craw, D., Chamberlain, C.P., 1997. Structure and fluid migration in a late Cenozoic duplex system forming in the Main Divide in the central Southern Alps, New Zealand. New Zealand Journal of Geology and Geophysics 40, 359–373.

Craw, D., 1997. Fluid inclusion evidence for geothermal structure beneath the Southern Alps, New Zealand. New Zealand Journal of Geology and Geophysics 40, 43–52.

Craw, D., 1998. Structural boundaries and biotite and garnet "isograds" in the Otago and Alpine Schists, New Zealand. Journal of Metamorphic Geology 16, 395–402.

Craw, D., Rattenbury, M.S., Johnstone, R.D., 1994. Structures within greenschist facies Alpine Schist, central Southern Alps, New Zealand. New Zealand Journal of Geology and Geophysics 37, 101–111.

Davey, F.J., Henyey, T., Holbrook, W.S., Okaya, D.A., S, T., Melhuish, A., Henrys, S., Anderson, H., Eberhart-Phillips, D., McEvilly, T., Urhammer, R., Wu, F., Jiracek, G.R., Wannamaker, P.E., Caldwell, G., Christensen, N., 1998. Preliminary results from a geophysical study across a modern continent–continent collisional plate boundary — The Southern Alps, New Zealand. Tectonophysics 288, 221–235.

DeMets, C., Gordon, R.G., Argus, D.F., Stein, S., 1994. Effect of recent revisions to the geomagnetic reversal time scale on estimates of current plate motions. Geophysical Research Letters 21, 2191–2194.

Findlay, R.H., 1987. Structure and interpretation of the Alpine schists in Copeland and Cook River Valleys, South Island, New Zealand. New Zealand Journal of Geology and Geophysics 30, 117–138.

Findlay, R.H., Sporli, K.B., 1984. Structural Geology of the Mt. Cook Range and Main Divide, Hooker Valley region, New Zealand. New Zealand Journal of Geology and Geophysics 27, 257–276.

Gallagher, K., Brown, R., Johnson, C., 1998. Fission track analysis and its application to geological problems. Annual Review of Earth and Planetary Sciences 26, 519–572.

Ghosh, S.K., Ramberg, H., 1987. Reorientation of inclusions by a combination of pure shear and simple shear. Tectonophysics 34, 1–70.

Grapes, R.H., 1995. Uplift and exhumation of Alpine schist, Southern Alps, New Zealand: thermobarometric constraints. New Zealand Journal of Geology and Geophysics 38, 525–533.

Grapes, R.H., Watanabe, T., 1992. Metamorphism and uplift of the Alpine schist in the Franz Josef–Fox Glacier area of the Southern Alps, New Zealand. Journal of Metamorphic Geology 10, 171–180.

Grapes, R., Vry, J.K., 1999. Garnet compositions track early, later and latest phases of Alpine Schist metamorphism, Central Southern Alps, New Zealand. Geological Society of New Zealand Miscellaneous Publication 107A, 51.

Grapes, R., Little, T.A., Vry, J.K., 1998. Aspiring lithological association extended through Alpine Schist, Marlborough Schist and Wellington greywacke. Geological Society of New Zealand Miscellaneous Publication 101A, 151.

Grindley, G.W., 1963. Structure of the Alpine Schists of South Westland, Southern Alps, New Zealand. New Zealand Journal of Geology and Geophysics 6, 872–930.

Gunn, B.M., 1960. Structural features of the Alpine Schists of the Franz Josef–Fox Glacier region. New Zealand Journal of Geology and Geophysics 3, 287–308.

Hirth, G., Tullis, J., 1992. Dislocation creep regimes in quartz aggregates. Journal of Structural Geology 14, 145–160.

Hirth, G., Tullis, J., 1994. The brittle-plastic transition in experimentally deformed quartz aggregates. Journal of Geophysical Research 99, 11,731–11,747.

Hobbs, B.E., Means, W.D., Williams, P.F., 1982. The relationship between foliation and strain: an experimental investigation. Journal of Structural Geology 4, 411–428.

Holcombe, R.J., Little, T.A., 2001. A sensitive vorticity gauge using rotated porphyroblasts, and its application to rocks adjacent to the Alpine Fault, New Zealand. Journal of Structural Geology 23, 979–990.

Holm, D.K., Norris, R.J., Craw, D., 1989. Brittle and ductile deformation in a zone of rapid uplift: Central Southern Alps, New Zealand. Tectonics 8, 153–168.

Ilg, B.R., Little, T.A., 1999. Kinematic partitioning of transpressional elements in the Alpine Fault mylonite, New Zealand. Geological Society of America Abstracts with Programs 31 (7), A110.

Jiang, D., Lin, S., Williams, P.F., 2001. Deformation path in high-strain zones, with reference to slip-partitioning in transpressional plate-boundary regions. Journal of Structural Geology 23, 991–1005.

Kamp, P.K.K., 1997. Paleogeothermal gradient and deformation style. Pacific front of the Southern Alps Orogen: Constraints from fission track thermochronology. Tectonophysics 271, 37–58.

Kleffman, S., Davey, F., Melhuish, A., Okaya, D., Stern, T., team, S., 1998. Crustal structure in the central South Island, New Zealand, from the Lake Pukaki seismic experiment. New Zealand Journal of Geology and Geophysics 41, 39–49.

Koons, P.O., 1987. Some thermal and mechanical consequences of rapid uplift: An example from the Southern Alps, New Zealand. Earth and Planetary Science Letters 86, 307–319.

Koons, P.O., 1992. Two-sided orogen: collision and erosion from the sandbox to the Southern Alps of New Zealand. Geology 18, 679–682.

Koons, P.O., 1994. Three-dimensional critical wedges: tectonics and topography in oblique collisional orogens. Journal of Geophysical Research 99, 12,301–12,315.

Leitner, B., Eberhart-Phillips, D., 1998. A focused look at the central Alpine Fault: Seismicity, focal mechanisms, and stress observations. Geological Society of New Zealand Miscellaneous Publication 101A, 143.

Lillie, A.R., Gunn, B.M., 1964. Steeply plunging folds in the Sealy Range, Southern Alps. New Zealand Journal of Geology and Geophysics 7, 403–423.

Lillie, A.R., Gunn, B.M., Robinson, P., 1957. Structural observations in central Alpine region of New Zealand. Royal Society of New Zealand Transactions 85, 113–129.

Lister, G.S., Snoke, A.W., 1984. S–C mylonites. Journal of Structural Geology 6, 617–638.

Little, T.A., Holcombe, R.J., Ilg, B.R., 2002. Kinematics of oblique continental collision inferred from ductile microstructures and strain in mid-crustal Alpine Schist, central South Island, New Zealand. Journal of Structural Geology 24, 219–239.

Luneburg, C.M., Lebit, H.D.W., 1998. The development of a single cleavage in an area of repeated folding. Journal of Structural Geology 20, 1531–1548.

Mason, B., 1962. Metamorphism in the Southern Alps of New Zealand. Bulletin of the American Museum of Natural History 123, 217–248.

Means, W.D., 1981. The concept of the steady-state foliation. Tectonophysics 78, 179–199.

Molnar, P., Anderson, H.J., Audoine, E., Eberhart-Phillips, D., Gledhill, K.R., Klosko, E.R., McEvilly, T.V., Okaya, D., Savage, M.K., Stern, T., Wu, F.T., 1999. Continuous deformation versus faulting through the continental lithosphere of New Zealand. Science 286, 516–519.

Mortimer, N., 1993. Jurassic tectonic history of the Otago Schist, New Zealand. Tectonics 12, 237–244.

Mount, V.S., Suppe, J., 1992. Present-day stress orientations adjacent to active strike-slip faults: California and Sumatra. Journal of Geophysical Research 97, 11,995–12,013.

Norris, R.J., Craw, D., 1987. Aspiring terrane: an oceanic assemblage from New Zealand and its implications for Mesozoic terrane accretion in the

Southwest Pacific. In: Leitch, E.C., Scheibner, E. (Eds.). Terrane Accretion in Orogenic Belts. , pp. 169–177 A.G.U. Geodynamic Series 19.

Norris, R.J., Bishop, D.G., 1990. Deformed conglomerates and textural zones in the Otago schists, South Island, New Zealand. Tectonophysics 174, 331–349.

Norris, R.J., Cooper, A.F., 1995. Origin of small-scale segmentation and transpressional thrusting along the Alpine Fault, New Zealand. Geological Society of America Bulletin 107, 231–240.

Norris, R.J., Cooper, A.F., 1997. Erosional control on the structural evolution of a transpressional thrust complex on the Alpine Fault, New Zealand. Journal of Structural Geology 19, 1323–1342.

Norris, R.J., Koons, P.O., Cooper, A.F., 1990. The obliquely convergent plate boundary in the South Island of New Zealand: implications for ancient collision zones. Journal of Structural Geology 12, 715–726.

Passchier, C.W., Trouw, R.A.J., 1996. Microtectonics. Springer, Berlin.

Platt, J.P., Vissars, R.L.M., 1980. Extensional structures in anisotropic rocks. Journal of Structural Geology 2, 397–410.

Prior, D.J., 1993. Sub-critical fracture and associated retrogression of garnet during mylonitic deformation. Contributions to Mineralogy and Petrology 113, 545–556.

Ramsay, J.G., 1967. Folding and Fracturing of Rocks. McGraw-Hill, New York.

Shi, Y., Allis, R.G., Davey, F.J., 1996. Thermal modelling of the Southern Alps, New Zealand. Pure and Applied Geophysics 146, 469–501.

Sibson, R.H., White, S.H., Atkinson, B.K., 1981. Structure and distribution of fault rocks in the Alpine Fault Zone, New Zealand. Geological Society of London Special Publication 9, 197–210.

Simpson, G.D., Cooper, A.F., Norris, R.J., Turnbull, I.M., 1994. Late Quaternary evolution of the Alpine Fault Zone at Paringa, South Westland, New Zealand. New Zealand Journal of Geology and Geophysics 37, 49–58.

Sporli, K.B., Lillie, A.R., 1974. Geology of the Torlesse Supergroup in the northern Ben Ohau Range, Canterbury, New Zealand. New Zealand Journal of Geology and Geophysics 17, 115–141.

Stern, T.A., Wannamaker, P.E., Eberhart-Phillips, D., Okaya, D., Davey, F.J., team, S., 1997. Mountain building and active deformation studied in New Zealand. EOS 78 (32), 329–336.

Stern, T., Kleffman, S., Scherwath, M., Okaya, D., Bannister, S., 2001. Low seismic wave speeds and enhanced fluid pressure beneath the Southern Alps of New Zealand. Geology in press.

Sutherland, R., 1995. The Australia–Pacific boundary and Cenozoic plate motions in the SW Pacific: Some constraints from Geosat data. Tectonics 14, 819–831.

Sutherland, R., Norris, R.J., 1995. Late Quaternary displacement rate, paleoseismicity, and geomorphic evolution of the Alpine Fault: evidence from Hokuri Creek, South Westland. New Zealand Journal of Geology and Geophysics 38, 419–430.

Teagle, D.A.H., Hall, C.M., Cox, S.C., Craw, D., 1998. Ar/Ar dating and uplift rate of hydrothermal minerals in the Southern Alps. New Zealand. In: Arehart, G.B., Hulston, J.R. (Eds.), Water–Rock Interaction. Balkema, Rotterdam, pp. 801–804.

Teyssier, C., Tikoff, B., Markley, M., 1995. Oblique plate motion and continental tectonics. Geology 23, 447–450.

Tikoff, B., Fossen, H., 1995. The limitations of three-dimensional kinematic vorticity analysis. Journal of Structural Geology 17, 1771–1784.

Tikoff, B., Fossen, H., 1999. Three-dimensional reference deformations and strain facies. Journal of Structural Geology 21, 1497–1512.

Tippet, J.M., Kamp, P.J.J., 1993. Fission track analysis of late Cenozoic vertical kinematics of continental Pacific crust, South Island, New Zealand. Journal of Geophysical Research 98, 16,119–16,148.

Treagus, J.E., Treagus, S.H., 1981. Folds and the strain ellipsoid: a general model. Journal of Structural Geology 3, 1–17.

Upton, P., 1995. Deformation-induced reaction in the Alpine Fault mylonites, Southern Alps, New Zealand. Geological Society of Australia Abstracts 40, 164.

Vry, J.K., Maas, R., Little, T.A., Phillips, D., Grapes, R., Dixon, M., 2001. Zoned (Cretaceous and Cenozoic) garnets and the timing of high grade metamorphism, Southern Alps, New Zealand. Journal of Metamorphic Geology, in review.

Walcott, R.I., 1998. Modes of oblique compression: Late Cenozoic tectonics of the South Island of New Zealand. Reviews of Geophysics 36, 1–26.

Walker, N.W., Mortimer, N., 1999. Dating high-grade metamorphic mineral growth in the Haast schist using U–Pb TIMS. Geological Society of New Zealand Miscellaneous Publication 107A, 167.

Wannamaker, P.E., Jiracek, G.R., Stodt, J.A., Caldwell, T.G., Gonzalez, V.M., McKnight, J.D., Porter, A.D., 2001. Fluid generation and pathways beneath an active compressional orogen, the New Zealand Southern Alps, inferred from magnetotelluric data. Geophysical Journal International, in press.

Wellman, H.W., 1979. An uplift map for the South Island of New Zealand, and a model for the uplift of the Southern Alps. Royal Society of New Zealand Bulletin 18, 13–20.

Wightman, R., 2000. The fabrics and ductile microstructures in the Alpine Schist and mylonite zone near Fox Glacier, New Zealand. B.Sc. (Hon) thesis, Victoria University of Wellington, 115pp.

Williams, P.F., 1976. Relationships between axial plane foliations and strain. Tectonophysics 30, 181–196.

Williams, P.F., Price, G.P., 1990. Origin of kink-bands and shear-band cleavage in shear zones: an experimental study. Journal of Structural Geology 12, 145–164.

Wright, T.O., Henderson, J.R., 1992. Volume loss during cleavage formation in the Meguma Group, Nova Scotia, Canada. Journal of Structural Geology 14, 281–290.